Transforming Microtubules into Microshuttles for Advanced Immunoassay Applications

by

Jenna Marie Campbell

A dissertation submitted in partial fulfillment
of the requirements for the degree of
Doctor of Philosophy
(Mechanical Engineering)
in the University of Michigan
2014

Doctoral Committee:

Professor Edgar Meyhöfer, Chair
Assistant Professor Barry Grant
Assistant Professor Ajit P. Joglekar
Professor Katsuo Kurabayashi

© Jenna Campbell 2014
All Rights Reserved

For Lisa Orr and Vivek Tomer—

For pushing me forward every time I wanted to take a step back.

Your love, support, and guidance have been invaluable.

ACKNOWLEDGEMENTS

This dissertation is the culmination of many years of work, which would not have been possible without the guidance of my advisor, Edgar Meyhöfer. He challenged me, taught me how to ask questions, and how to "do science." Always having an open door, your support and expertise has been invaluable academically, professionally, and personally.

I would also like to acknowledge Katsuo Kurabayashi for your expertise and support. Our meetings gave me a broader perspective on our projects, which played a large role in shaping my academic and professional goals. Committee members Ajit Joglekar and Barry Grant have always been generous with their time, and I am thankful for the advice and expertise they have given throughout my graduate career. My co-workers Charles Jiang and Neha Kaul played a critical role in this work. Thank you for bringing laughter along with great insight into my work.

I would like to acknowledge Professor James Gole for encouraging me to continue my education, which brought me to the University of Michigan. I would not have discovered my love of science and research if it were not for your passion to inspire undergraduates and educate young scientists.

Finally, my friends and family who have supported me have been critical to my accomplishments over the last five years. Vivek Tomer has given me guidance, advice, and support that was so helpful in overcoming every hurdle I encountered at Michigan. Megan Roberts and Marilyn Gatewood are two brilliant female engineers that I am fortunate to have as role models and friends. My greatest thanks goes to Lisa, Casey, Claire, and Hannah whose patience, love, and support have carried me through my whole life and will take me through many more years.

TABLE OF CONTENTS

DEDICATION ii

ACKNOWLEDGEMENTS iii

LIST OF FIGURES vii

LIST OF TABLES viii

LIST OF ABBREVIATIONS ix

CHAPTER 1: MOTIVATION 1

CHAPTER 2: BACKGROUND 3

2.1 Microtubule-Kinesin Systems: From *In* Vivo Motility to Lab on a Chip 3

Microtubules as Nanoshuttles 5

Highly Engineered Cargos 7

Kinesin Motor Control 8

Mechanical Control of Microtubules 10

Electrophoretic and Magnetic Control of Microtubules 12

2.2 Proteomic Biosensors 13

2.3 Kinesin-Driven Immunoassay Platform 17

Microtubule Concentrator 17

Motivation and Potential for Immunoassay Applications 19

Hurdles in Combining Kinesin and Microtubules in Proteomic Sensors 20

CHAPTER 3: ANTIBODY-FUNCTIONALIZED NANOSHUTTLES DRIVEN BY BIOMOLECULAR MOTORS FOR SENSITIVE IMMUNOASSAY APPLICATIONS 24

3.1 Introduction 25

3.2 Approach 2

3.3 Results....28
Specificity and Binding Capacity of Antibody-Functionalized Microshuttles....28
Motility Properties of Antibody-Functionalized Microshuttles....36
Limitations for Sandwich Assay Construct....37
3.4 Conclusions....41
3.3 Experimental Section....42
Microtubule Preparation....42
Kinesin Purification....43
Microtubule Antibody Conjugation....43
Ellman's Reagent Assays....44
Binding Capacity Assays....45
Motility Assays....46

CHAPTER 4: KINESIN AND MICROTUBULE COMPATABILITY IN HUMAN URINE, SALIVA, AND BLOOD PLASMA....47
4.1 Introduction....47
4.2 Biotinylated Microtubules and Their Ability to Bind Streptavidin Cargos in Human Urine, Saliva, and Blood Plasma....49
4.3 Microtubules and Their Motility Properties in Human Urine, Saliva, and Blood Plasma....55
4.4 Motility Characteristics Required for Steering Microtubules in Kinesin-Driven Technologies....57
4.5 Motility Properties of Kinesin and Microtubules in Human Blood Plasma....64
Unfiltered Blood Plasma....65
Filtered (10 kDa) Blood Plasma....69
4.6 Conclusions....71
4.7 Experimental Section....72
Human Sample Preparation: Blood Plasma....72
Human Sample Preparation: Saliva....73
Human Sample Preparation: Urine....73

Microtubule Preparation....74
Binding Capacity Assays....75
Quality of Motility....76

CHAPTER 5: CONCLUSIONS AND FUTURE WORK....77
5.1 Conclusions....77
5.2 Future Work: Fluorescent Detection Via Labeled Detection Antibodies....79
Modifying Assay Geometry to Support the Transport of Large Cargos....80
Modifying MT-Antibody Conjugation Procedure to Support the Transport of Large Cargos....81
Transport Fewer, Larger Cargos to Sustain Motility....84
5.3 Future Work: Kinesin-Driven Immunassay Platforms in Blood Plasma....84
Separate Sample Collection from Gliding Assays....85
Engineer Technologies Accommodating for Motility in Blood Plasma....86
5.4 Future Outlook for Kinesin-Driven Technologies....88

WORKS CITED....90

LIST OF FIGURES

Figure 2.1 Geometry of gliding assay…..……..……..…….. 5
Figure 2.2 Microtubule being guided mechanically……...……. 11
Figure 2.3 ELISA assays……...……...……. 14
Figure 2.4 Microtubule concentrator device……....……. 18
Figure 3.1 Conjugation protocol……. 27
Figure 3.2 Schematic representation of binding assay……...……. 29
Figure 3.3 Antigen specific binding and binding capacity……. 31
Figure 3.4 Image processing for binding capacity measurements…….……... 33
Figure 3.5 Functionalized microtubules support motility…...……..……. 37
Figure 3.6 Effect of antibody sandwich cargo on kinesin-microtubule gliding assay……... 40
Figure 4.1 Microtubules binding TMR-streptavidin cargos in body fluids……. 53
Figure 4.2 Gliding assay velocities in body fluids……...……..... 56
Figure 4.3 High quality motility and the effects of aggregation…...……. 59
Figure 4.4 Floating ends are detrimental to guiding microtubules……..……. 62
Figure 4.5 Gliding assay motility in blood plasma…...……..……. 66
Figure 4.6 Gliding assay motility in 10 kDa filtered blood plasma…..……. 70

LIST OF TABLES

Table 1 Competitive immunoassay formats and assay conditions…….……. 16
Table 2 Profiles of body fluids commonly used for diagnostic tests……. 21

LIST OF ABBREVIATIONS

Ab	Antibody
AMPPNP	Adenylyl-imidodiphosphate
ATP	Adenosine triphosphate
BSA	Bovine serum albumin
Bt	Biotin
CSF	Cerebral spinal fluid
Cy5	Cyanine-5
DNA	Deoxyribonucleic acid
DTT	Dithiothrietol
GTP	Guanosine triphosphate
IL-6	Interleukin-6
kDa	Kilodalton
LOC	Lab on a chip
MT	Microtubule
PBS	Phosphate-buffered saline
PCR	Polymerase chain reaction
PIPES	Piperazine-N,N'-bis(2-ethanesulfonic acid)
POC	Point of care
SDS-PAGE	Sodium dodecyl sulfate-polyacrylamide gel electrophoresis
SMCC	Succinimidyl-4-(N-maleimidomethyl)cyclohexane-1-carboxylate
SPR	Surface plasmon resonance
STV	Streptavidin
TMR	Tetramethylrhodamine

CHAPTER 1

MOTIVATION

Advances in clinical diagnostics and health care critically depend on new tools to efficiently and reliably analyze complex patterns of bio- and disease markers. There is significant evidence that proteomic approaches to analyze arrays of biomarkers are very effective in early disease detection including cancers, and low budget, point-of-care proteomic sample analysis would be beneficial in improving global health care.[1-7] Currently, enzyme-linked immunosorbent assays (ELISA) are the most common protein analysis methods, but their sensitivity is usually limited by some relative threshold concentration (1-10pM) that, in some cases, is too high to detect early stages of disease progression.[8, 9] Since no protein amplification techniques exist, analogous to polymerase chain reactions for DNA, surpassing this threshold concentration (1-10pM) is difficult.[10],[11-13] The ultimate objective of my dissertation is to progress an innovative ELISA-based nanotechnology that allows for rapid capture and specific transport of biomolecules using a single, small (nanofluidic) sample volume and limited manual labor without the need of an external power source.

The nanotechnology is an engineered protein system that takes advantage of the kinesin and microtubule system that nature has taken the time to develop. Only for the last several decades have researchers been exploring the potential

the cytoskeletal transport systems have *in vitro* and in lab on chip technologies. Here, I bridge the gap in knowledge that exists in taking the kinesin-microtubule system out of biological cells and into advanced lab on chip ELISA-based diagnostic devices for point of care applications. With progress in the fields of nano- and microfluidics and bioengineering being key to progressing medical, point if care diagnostic devices, the development of nanoscopic ELISA platforms that are capable of capturing and detecting ultralow concentrations of proteins is essential in further advancing these medical technologies.

Leveraging cytoskeletal transport systems for microscopic transport systems that are highly regulated in biological cells brings a significant advantage when compared with entirely man-made systems. In such protein-based systems, biologists and engineers can work in parallel to advance our understanding of the regulation mechanisms of the system and, therefore, contribute to advancing autonomous regulation mechanisms in lab on chip devices. Biological discoveries relating to the specificity of the cytoskeletal transport system can be incorporated into such a device eventually turning it into a "smart" device guided by nature's protein regulation mechanisms.[14]

Implementing a protein analysis requiring a small sample volume at very low cost will reduce trauma to more sensitive patients and allow for future biomolecular motor-driven technologies to serve as a low budget, bed-side health diagnosis tool having global health care applications. As such technologies progress, they will facilitate a paradigm shift, particularly in detection of the early onset of diseases and continuous health monitoring

CHAPTER 2

BACKGROUND

In this chapter I will begin by discussing the previous work that has been done over the last two decades in taking the kinesin and microtubule system out of a cell and into *in vitro* systems. I will discuss the advances scientists and engineers have made in modifying the protein system to transport specific cargos and control and regulate its motility. The previous work will be framed to highlight the future potential the kinesin-microtubule system has to be integrated into lab on a chip technologies and, specifically, point of care medical diagnostic devices. Then, I will look at the current demands for medical diagnostic devices and the approaches others have taken to engineer technologies that satisfy those demands. Culminating these two topics, I will conclude with a more specific example as to how the kinesin-microtubule system can be integrated into micro- or nanofluidic devices and be engineered to satisfy the demands for point of care, lab on chip proteomic detectors for sensitive diagnostic tests.

2.1 Microtubule-Kinesin Systems: From *In Vivo* Motility to Lab on a Chip

During the last decade many advances have been made in revealing the complexities of the nano- and microscale systems existing in biological cells.

Progress has been made in getting these systems to function in *in vitro* environments where they can be studied as independent systems. Due to their robustness *in vitro* and nanoscopic properties, several of these protein systems often serve as an inspiration for nano and micro technologies.[14-19] One system of particular interest is the active transport system present in eukaryotic cells. Here, organized networks of microtubules and actin filaments in the cytoskeleton of a cell provide tracks for a variety of biomolecular motors, such as kinesins, to move along and generate mechanical forces. These motor molecules power cellular mechanical processes including cell contraction and movement, mitosis, and intracellular transport by directly converting chemical energy (hydrolysis of ATP) into mechanical work.[20, 21] Adenosine triphosphate (ATP) powers the stepping motion of kinesin. The chemical energy extracted from the hydrolysis of ATP in this kinesin ATPase is converted to mechanical work as the motor molecule steps along the microtubule protofilament. The motor protein kinesin is responsible for intracellular transport and has many properties that have attracted considerable interest in these molecules as energy transducers and transport systems for nanotechnology applications.[15, 22] Kinesins are nanoscopic, move processively along MTs for micrometer-long distances, support high speed (several μm/s), use little energy, and the microtubules (MTs) kinesin travel along are stable, robust tracks that can be readily engineered into artificial lab on a chip devices. [14, 15, 18, 23-31]

While studying kinesin-MT systems in *in vitro* environments, a typical assay will take place in a microfluidic chamber. Kinesin motor molecules nonspecifically bind to the surface of the chamber. A motility buffer containing

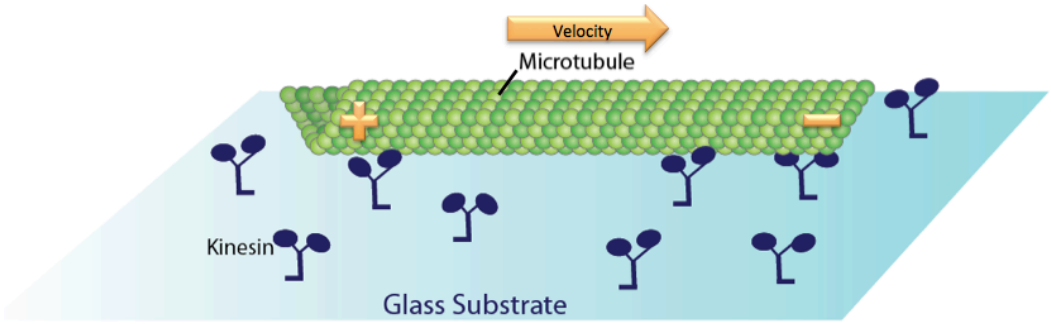

Figure 2.1 Geometry of a gliding assay. Plus-end directed motors step along the MT surface towards the plus end to propel the MT along the glass surface.

ATP and MTs is then flown into the chamber. The kinesin motor domain exposed to the ATP-containing motility buffer binds to MTs free in solution. Kinesin motors step along the MTs with an inherent directionality. As illustrated in **Figure 2.1**, when all of the kinesin step in the same direction along the MT, the kinesin motor molecules push MT along the kinesin-coated surface of the microfluidic chamber. This is known as a gliding assay. MTs can glide along the surface uninterrupted for several millimeters at speeds >1 μm/sec without any external pumps or power sources. These qualities and the scale of the system are ideal for active transport in microfluidic systems.

Microtubules as Nanoshuttles

Due to the appealing active transport mechanism the MT-kinesin system provides *in vitro*, there have been a number attempts to functionalize microtubules as it appears to be the simplest way to adapt this protein system into a useful active transport mechanism in microfluidic, lab on chip (LOC) systems.[24, 32] The first cargos carried utilized biotinylated tubulin and the strong biotin-streptavidin (Bt-STV) linkage.[33] Streptavidin is multivalent, so a Bt-STV-

Bt sandwich is easy and inexpensive to create. These Bt-STV functionalized MTs have been utilized to transport and even manipulate biotinylated DNA using a Bt-STV-Bt linkage.[34-37] Biotinylated nanospheres, quantum dots and microspheres all served as cargoes on biotinylated MTs.[38-40] Once this MT-Bt-STV-Bt-cargo linkage was optimized, the next logical step was to use this modified tubulin to attach biotinylated antibodies to microtubules to transport specific proteins.[41, 42] These conjugations brought about a lot of excitement as they introduced the kinesin-microtubule system into potential immunoassay platforms.

The major disadvantage to the Bt-STV-Bt linkage is undesired crosslinking that is possible due to the multivalent properties of STV. The assay must be carefully done in many sequential steps to reduce the number of undesired MT-MT, cargo-cargo, or MT-cargo-MT crosslinking events that result in clusters of undesired byproducts. Some researchers purposely crosslinked microtubules in a controlled manner using the Bt-STV-Bt linkage to create clusters of microtubules in different geometries such as linear nanowires or nanospools.[43, 44] However, the future applications for such geometries are still unclear. Later on, a variety of more specific conjugation techniques were developed to covalently link antibodies to microtubules using homo- or heterobifunctional crosslinkers.[45, 46] While these techniques are an improvement to the biotin-dependent alternatives, most still leave room for undesirable cross-linked products similar to the Bt-STV linkage.

As these MT microshuttles evolved, the LOC kinesin-driven platforms also had to advance in hopes to effectively incorporate these systems into useful devices. Here, I will discuss the different ways researchers have manipulated this

transport system and engineered devices to accommodate the controllable properties of kinesin and microtubules. It remains largely unclear how biological cells control the chemo-mechanical activity of kinesin motors to achieve the complex and specific transport properties present in cellular function.[47-52] Theoretically, if the underlying control mechanisms that drive this highly regulated intracellular transport were completely understood, one could create and control a highly specific, infinitely multiplexed device that relies solely on proteins and protein modifications to deliver cargos. Since these control mechanisms are not fully understood, it is not clear how kinesin and microtubules can be harnessed to their fullest potential for specific multidirectional micro transport. Several attempts have been made to overcome this limitation by utilizing the inherent chemical and mechanical properties of the kinesin-microtubule system or engineering micro- or nanofabricated structures or "smart" polymers to have better control of this system, which are discussed further below. Significant strides in engineered biological systems must be made to further understand how fully take advantage of kinesin and microtubules in LOC technologies.

Highly Engineered Cargos

While significant work has been done to functionalize MTs, several groups have gone a step further in engineering cargos and tethers that collect, transport, and deliver cargos. Being able to control the transportation or delivery of micro or nanoscaled cargo is ideal in microreactors, concentrators, or targeted activation. All of the developed techniques incorporate engineered DNA primers. Complimentary DNA primers linked to the MT and the cargo enable

pick up, and a more preferential complementary primer is exposed on the delivery site with the purpose of pulling the cargo off of the microtubule. Brunner, *et al.* developed a microfabricated surface that enabled crossing MTs to pick up treated microspheres with DNA tethers.[53] The Vogel and Sutoh group went beyond by gathering, transporting, and delivering a specific analyte to a deposition region using complementary DNA mentioned previously.[54, 55] While successful, this requires a highly engineered cargo, which is not desirable for broad medical diagnostic purposes that typically depend on a huge library of antibodies for proteomic detection but may be reasonable for other micro scale applications.[56-60]

Kinesin Motor Control

While our knowledge of what naturally controls kinesin motors in biological cells is limited, many have taken the most basic understandings of kinesin motors and engineered systems that can turn motility on and off in gliding assays. Controlling the accessibility of ATP in solution can regulate motility. This concept has been utilized by developing stimuli-responsive polymers to cage ATP.[61] Rahim, *et al*. and Hess, *et al.* used ATP caged by a photoresponsive polymer that releases ATP into the microfluidic chamber after being exposed to an ultraviolet pulse.[62, 63] The Diez group used a thermo responsive polymer to create a similar reversible stop and go motility control in a gliding assay format. Instead of controlling the ATP in solution, this polymer could be activated to block kinesin motor domains and prevent MTs from binding and traveling along the kinesin surface. The polymer is nonspecifically adsorbed to the substrate alongside kinesin motors. When cooled to 27°C, the

polymer expands and physically blocks access to the motor domain, preventing MT-kinesin interactions. When heated to 35°C the polymer finds a more preferable conformation, tangled closer to the glass surface and exposes the kinesin heads to the MT containing motility buffer.[61] Recently, Diez also engineered the opposite configuration to create controlled motility where the polymer was bound to the MT instead of the kinesin surface.[64] The rate of kinesn's ATPase activity increases at higher temperatures thus supporting a proportionately higher velocity. Unfortunately, the variation in kinesin activity is not significant enough to use as a robust signal, so using these dynamic thermo-responsive polymers is advantageous at functional temperature ranges.[65-67] Taking control over the motor molecule, the Bachand group engineered a kinesin motor that contained a divalent metal binding site in the neck linker region. Exposing motors to a solution containing divalent metal ions inhibits kinesin, thus preventing motility. The inhibition can be reversed by introducing a number of chelating agents into the system.[68]

Engineering the kinesin to exhibit desirable characteristics is a timely and expensive endeavor, but with the improvement of computational modeling, highly engineered motors may not be too far away.[69, 70] Since motors are the backbone to active, directed intracellular transport *in vivo,* looking at engineered and natural motor control mechanisms is ideal for making these nano-transport systems more complex and highly regulated *in vitro*. A lot of future potential lies in multiplexed and advanced cargo delivery by focusing on motor control.

Mechanical Control of Microtubules

Many attempts to mechanically control the directionality of microtubule movement have been made by utilizing the physical interaction between oncoming microtubules and barriers with which they interact. This work was pioneered by the Meyhöfer and Kurabayashi group where Lin, *et al.* developed a model that illustrates that the MT bends and is guided in the direction that is most energetically favorable when coming in contact with a kinesin-free wall (See **Figure 2.2**).[71, 72] In gliding assays microtubules can bend at angles smaller than that suggested by their persistence length because tens or hundreds of kinesin motors are applying a force that outweighs the Brownian motion that cause bending.[73] In these gliding assays a majority of the microtubule is bound to kinesin, but the very tip remains free and controls the directionality of the gliding motion. Without interference from a mechanical blockade, the tip, free of kinesin, is limited to bending due to thermal energy. In this model and experimentally, the direction in which the MT bends when it hits a kinesin-free wall depends on how the very tip of the microtubule is directed.[74]

This interaction is also dependent on the material properties of the wall.[75-78] If a MT approaches a wall coated with functional kinesin molecules, there is some probability the MT will travel over the wall dissociate from the kinesin-coated surface instead of being steered by the wall. Surfaces can be fabricated and treated to be unaccommodating to proteins binding which have been utilized to create physical barriers in microfluidic chambers. For example, an extremely hydrophobic surface will cause proteins to denature and become non-functional. Lin and others have used this mechanical steering of MTs with some blockade to autonomously guide MTs to specific regions or in a certain

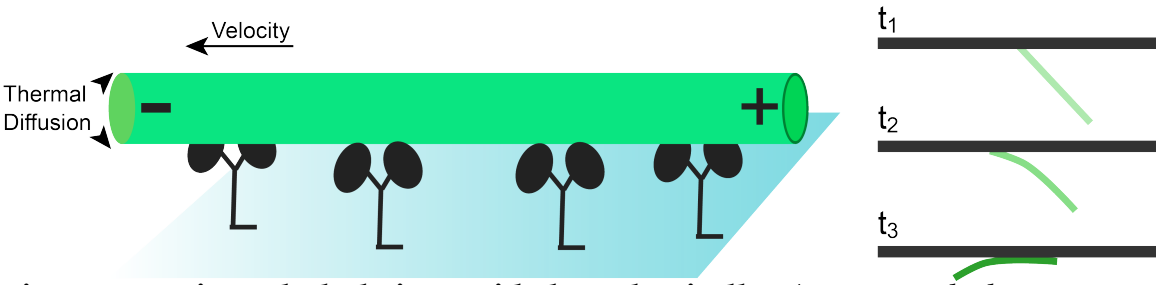

Figure 2.2 Microtubule being guided mechanically. As microtubules come in contact with a wall (*black line on right*), the thermally diffusing leading minus end (*left*) is guided in the direction that is most energetically favorable. As a result, the MT follows this motion and is steered by the wall as it glides forward (*right*).

direction.[77, 79-82] Specifically, the microfabrication process developed by Lin has become the typical standard for mechanically guiding MTs in micro- and nanofluidic systems.[79] CYTOP is deposited on a glass wafer and etched away using SF_6 reactive ion etching, exposing the glass surface. Under specific fabrication parameters, kinesin motors bind and support motility on the exposed glass surface. The CYTOP can be coated with a Pluronic polymer and then possess material properties that cause kinesin to denature and prevent motility on the CYTOP walls. These walls then serve as mechanical barriers that guide MTs throughout the glass channels.

Additional mechanical constraints can be placed on the system by interfering with the kinesin-MT binding. Many have studied the effects of coating MTs with nanoparticles, for example, and observed effects on motility.[83-85] One group engineered a microfabricated device to sort microtubules by length. Microtubule length can be controlled by adjusting the polymerization parameters during tubulin growth or by shearing stabilized microtubules with a Hamilton syringe or pipette tip.[86] The Sato group created a biased gradient of microtubules of different lengths by fabricating microtrenches that allow only MTs of a length greater than the width of the trench to cross. Shorter

microtubules fell off the ledge and could not bridge the gap to continue transport to the other side of the trench.[87] Engineering a system that sorts or guides microtubules mechanically lessens the importance of using highly modified proteins for controlling the system and supports autonomous control that is promising for multiplexing.

Electrophoretic and Magnetic Control of Microtubules

Microtubules have an inherent negative charge on their surface.[88] This charged surface is thought to be important in motor-MT binding events.[69, 70] Many have utilized this negative charge by guiding, aligning or manipulating MTs using electrophoresis.[32, 88-90] Van den Heuvel, *et al.* implemented electrophoresis into a concentrator device to separate MTs at a Y-junction with two different fluorescent labels.[89] A charge was applied across a Y-junction to either attract or repel MTs to the appropriate channel. While successful, this approach requires constant surveillance of incoming filaments at a single Y-junction, a large and expensive research microscope, and has low throughput. Microtubules have also been aligned and manipulated using dielectrophoresis, and, additionally, using a magnetic field after magnetic particles were attached to one end of the MT.[91, 92] While the previous work utilizing dielectro- and electrophoresis is binary (attraction or repulsion, alignment or randomization), this technique has potential in multiplexing kinesin-driven devices. Changing the surface charge of a microtubule or conjugating a material with different dielectrophoretic properties would allow researchers to tune and multiplex a device steered by an electric field. Although, a potential hurdle is that changing

the surface properties of the MTs may affect the kinesin interactions and impair motility.

While there has been great development in manipulating and controlling this cytoskeletal system *in vitro*, the only successful attempts at autonomously multiplexing a device were done by sorting MTs by length. The advances that have been made in utilizing the kinesin-microtubule system in more applied LOC technologies looks promising. Like many LOC systems that incorporate biological systems, the desire to miniaturize medical devices, including diagnostic devices, and transform them into smaller point of care (POC) technologies that are easier to use and more reliable is desired. In the following section, I discuss recent advances in microfluidics and immunoassays and how they benefit future point of care diagnostics. Then, I will assess how the work done with the kinesin-microtubule system can merge with the demands of proteomic biosensors which motivates the foundation of my dissertation, developing a kinesin-driven ultrasensitive immunoassay platform.

2.2 Proteomic Biosensors

The current demand in the field of proteomic biosensors is to develop a more sensitive, less invasive, inexpensive, rapid diagnostic device.[93-95] The most commonly used proteomic detection mechanism is an enzyme-linked immunosorbent assay (ELISA) (See **Figure 2.3**). ELISA assays are typically performed on a plate containing several wells. In direct ELISA assays the base of each well is coated with a capturing antibody that specifically captures a protein of interest. The unbound sample is rinsed from the well and a detection antibody

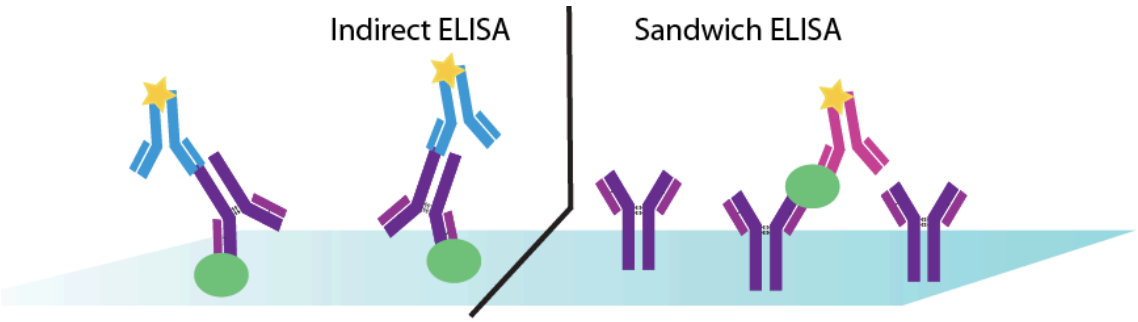

Figure 2.3 ELISA assays. Capturing antibodies (*purple*) specifically bind to protein antigen. A detection antibody that is fluorescently labeled is either complimentary and binds the protein of interest (*pink*) or secondary and binds the end of the detection antibody (*blue*).

is flown in. The fluorescently tagged detection antibody is complementary to the antigen and binds to the analyte that was initially captured by the capturing antibody, forming an antibody sandwich. In an indirect ELISA assay protein is nonspecifically adsorbed to the base of the well along with the other proteins in the sample. The capturing antibody binds only the protein of interest, or antigen, in the well. The detection antibody in indirect ELISA is a secondary antibody that binds to the heavy chain of the capturing antibody. The signal from the label on the detection antibody is measured, and this signal corresponds to the amount of analyte in the initial sample. These assays have a typical detection limit of 1-100 pM which is limited by either the sensitivity of the fluorescent measurement or the affinity of the analyte to the antibody.[96] While there has been a significant amount of effort to improve the affinity of antibodies to reach affinities on the order of a femtomolar, this is an extremely expensive and timely endeavor and is generally not used for improving the sensitivity of these assays for a wide variety of biomarkers.[97-106] Thus, to improve the sensitivity of proteomic biosensors and maintain an affordable cost for patients, other technologies have been developed to challenge the typical well-based ELISA approach. Common techniques

employed by technologies used today to surpass the standard ELISA limitations include the following:

- **Lower detection limits**: Increase the signal to nose ratio for fluorescence or rely on other, more sensitive detection methods apart from fluorescence or amplify the analyte signal.
- **Faster assays**: Allow antibody to diffuse within the sample instead of relying on the diffusion of analyte to an antibody-coated surface.
- **More accurate tests limiting error**: Create an autonomous lab on a chip device that reduces human error.
- **Reduce costs and invasiveness of test**: Downsize to nano- or microfluidic systems that require smaller sample and reagent volumes to lower costs. Smaller samples are less invasive to sensitive patients such as newborns. Less invasive tests permit more frequent testing or monitoring the progression of diseases or therapies.[107]

Table 1 shows comparisons between typical ELISA well assays and competing approaches that currently exist on the market and their assay specifications. Notice the tradeoffs in each technology. Some improve the detection limit but lack ease of use or specificity while others improve ease of use and have comparable detection limits. Trade offs exist for all of these technologies being developed. As seen in the table below, progress has been made in engineering and manipulating microfluidic immunoassay platforms to reach lower detection

Assay	Assay Description	Detection Limit	Sample Volume	Assay Time	Source	Notes
ELISA	Sandwich assay in a well. Fluorescent detection signal from either a secondary or complementary detection antibody containing fluorophore.	1-10 pM	10 μL	4-6 hours	[65, 108]	• Multiplexed • Most widely accepted diagnostic currently used in Western medicine • Femtomolar detection possible with engineered, high affinity antibodies
Magnetic Bead Concentrators	Antibody-functionalized paramagnetic beads are suspended in sample and concentrated with a magnet. Fluorescent detection from detection antibody containing a fluorophore.	1 pM	2.5 μL	30 min.	[109, 110]	• Not diffusion limited • Fast • Easy to use in protein-rich body fluid samples • Characterizing the result is an extra step
Surface Plasmon Resonance (SPR)	Protein binds to gold surface that was functionalized with antibodies. The bound mass changes the SPR. Antibodies are necessary to get a protein-specific signal.	1 pM	100 μL	30 min.	[111]	• *In situ* detection • Expensive: $500K initial investment plus ~$40 for each chip • Not reliable for complicated samples
Rolling Circle Amplification	After a sandwich assay completely binds to the analyte, the detection antibody contains DNA primer instead of a fluorophore. A complimentary DNA circle binds to primer. With DNAse in solution, DNA is polymerized from circle template with fluorescent nucleotides. Final fluorescent signal from nucleotides correlates to amount of detection antibody bound.	3 aM	10 μL	3 hours	[11], [13]	• Detection antibody is highly engineered • Analyte is unaltered • Ultra low detection capable by amplifying the detection signal via DNA amplification • Not commercialized, technically challenging to reproduce
Immuno-Chromatographic Strips	Sample is placed on the end of a strip and moves through the strip by capillary forces. Some binary response is given either by agglutination, a labeled detection conjugate, *etc.* to detect the analyte.	10 pM	500 μL to several mL	30 min.	[11, 94, 112]	• Disposable, point-of-care device that does not require advanced facilities • Stable in ambient temperatures • Some sample purification or treatment required • Binary signal limits diagnostic capabilities

Table 1 Competitive immunoassay formats and assay conditions

limits, lower costs, reduce human induced error, and reduce assay time. While microfluidics had a role in accomplishing all of these tasks, existing methods to significantly reduce the detection limit that rely on bioengineering, such as the rolling circle amplification and engineered high affinity antibodies, are often too expensive and too highly engineered to translate into practical, broad, high throughput diagnostics. My dissertation work incorporates several of the concepts inspired by the above technologies along with the previously discussed potentials in incorporating the kinesin-MT system into LOC devices.

2.3 Kinesin-Driven Immunoassay Platforms

Microtubule Concentrator

Engineers have explored the various ways to manipulate the kinesin-microtubule system using their mechanical or electrostatic properties or altering biochemistries as discussed in Section 4.1. While these concepts have been fundamentally explored, it was not until the Meyhofer and Kurabayashi groups began integrating the kinesin-microtubule system into engineered microfluidic devices that the motor proteins looked promising for advanced, applied technologies. Taking what was known regarding mechanically steering microtubules, they designed a microtubule concentrator device powered by kinesin motor molecules that autonomously guided and trapped microtubules in a concentrator region.[72, 80]

The concentrator device illustrated in **Figure 2.4** is constructed using the aforementioned fabrication process that selectively promotes kinesin functionality in etched glass regions while CYTOP walls guide microtubules into

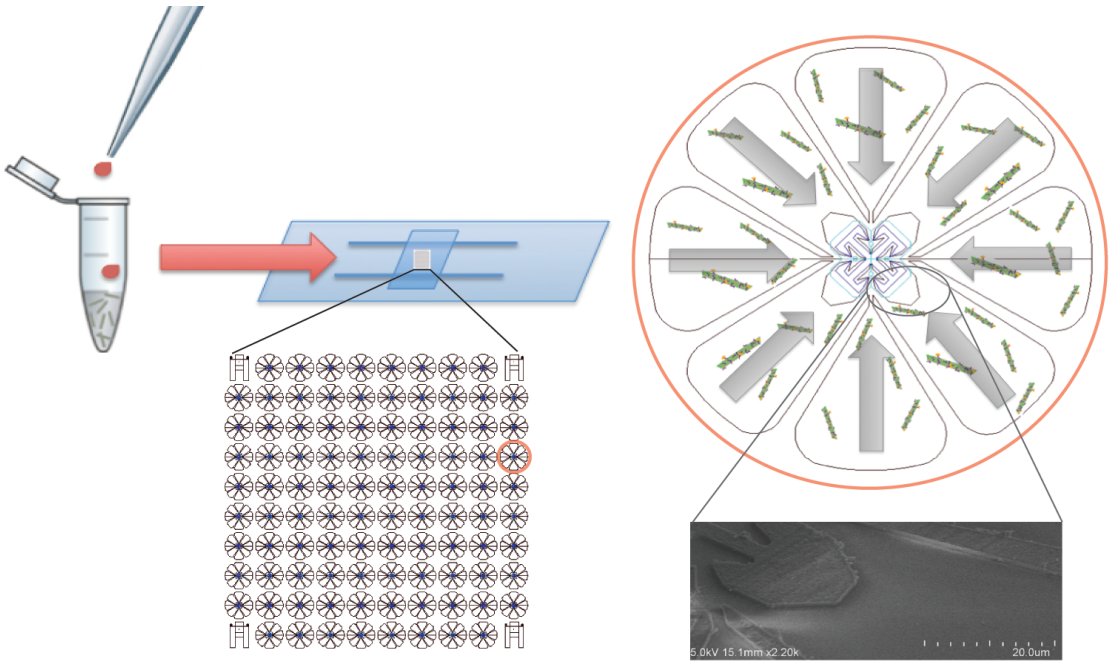

Figure 2.4 Microtubule concentrator device. The device is engineered to autonomously guide MTs to a center concentrator region (*top right*). Perpendicular CYTOP walls (*bottom right*) guide the MT tips that come in contact with the wall. To adapt the device for POC LOC diagnostic device, antibody functionalized MTs would incubate with the sample (*left*) and be concentrated in the device for detection. Figure adapted from Lin, *et al*. Nanoletters **8**(4), 2008.

a concentrator region. Microtubules land in the kinesin-coated, glass petal-shaped regions where they are transported by kinesin in a gliding assay. While the instantaneous directionality of the microtubules cannot be controlled, over time, the geometry of the curved CYTOP walls surrounding the petal regions guides the microtubules into the center of the device. As microtubules reach the center of the device, they enter into the concentrator region. The concentrator region is comprised of arrowhead, shaped glass surfaces that are covered with a parylene cover. The arrowhead regions, lined with CYTOP walls, cause the microtubules to serpentine within the concentrator region. If the microtubules disassociate from the glass (*xy*) surface, then the parylene cover prevents microtubules from escaping the concentrator region from the *z* direction. As a

result, millimeters of microtubules can enter into a microfluidic chamber and then be specifically concentrated into a 25 μm x 25 μm concentrator region in less than 30 minutes.

Motivation and Potential for Immunoassay Applications

Reflecting on the previous discussion in Section 4.2 on engineering advanced immunoassay platforms, concentrating analyte, working with small (<μL) sample volumes, and creating a diagnostic platform that is not complicated for the end user are all of interest in the field of medical diagnostics. Diagnostic devices for point-of-care (POC) applications have additional criterion including the following: working with non-invasive samples, requiring no ancillary equipment, and being easy to use. Using antibody functionalized microtubules as nanoshuttles that can collect and transport specific analytes combined with Liu's microtubule concentrator has great potential in advancing current immunoassay technologies.

Each concentrator requires only 0.13 nL of sample, concentrates millimeters of microtubules, and runs solely off of chemical energy (ATP). These traits coupled with antibody functionalized microtubules and an on-chip detection mechanism would make this system ideal for a potential POC diagnostic device. To transform this microtubule concentrator into an immunoassay platform, two critical gaps in knowledge must be addressed to realize its potential. First, the antigen binding capacity of the microtubules must be properly characterized using various biochemistry and protein characterization techniques to ensure that relevant detection capabilities can be

realized in the system. Second, all aspects of the system (kinesin, microtubules, motility, antibody-antigen binding, *etc*.) must not be compromised when immersed in medically relevant samples.

Hurdles in Combining Kinesin and Microtubules in Proteomic Sensors

Sustaining various protein functions in these relevant protein systems (kinesin, microtubules, antibody and antigen) in medically relevant biological samples is a hurdle that has yet to be addressed. Samples required for protein-based diagnostics include, but are not limited to, blood, urine, saliva, cerebrospinal fluid (CSF), and tissue extracts.[93] Cytoskeleton components including kinesin and microtubules are not inherently found in biological fluids; their natural environments are inside eukaryotic cells. In the proposed kinesin-driven immunoassay platform, motility and stability of the microtubule-kinesin construct must remain stable to concentrate antigen. Immersing kinesin and microtubules into protein-rich biological samples where they are not necessarily inherently compatible brings concern to their ability to remain motile and functioning because protein-protein interactions, whether they are specific or nonspecific, can be detrimental to *in vitro* assays. The complexity and diversity of such samples can be seen in **Table 2**. Due to the heterogeneity found in biological samples, it is unknown whether there are protein-protein interactions that will interfere with the kinesin-microtubule construct *in vitro*. Antibodies and their antigens, however, are found in abundance in blood samples. The antigenicity of antibodies and their antigens are found relatively unaffected when immersed in various biological fluids. They are manufactured, verified, and then commercially sold to clinicians to use in ELISA assays in various biological

Sample	pH	Protein Concentration (mg mL^{-1})	Ionic Strength (mmol L^{-1})	Commonly Used to Detect
Blood Plasma	7.3-7.5	50-70	145	Proteins, cholesterol, glucose, small molecule drugs
Urine	4.6-8.0	0.1-13.5	150-300	Hormones, small molecule drugs, blood cells
Saliva	6.2-7.7	0.7-2.5	44-163	Local (oral) microbes and proteins, DNA
Cerebrospinal Fluid	7.2-7.3	0.3-0.7	130-170	Neurological disorders, infection, neurological damage

Table 2 Profiles of body fluids commonly used for diagnostic tests[113-117]

samples. So, the biggest concern in incorporating biological samples into the microtubule concentrator device is whether the kinesin-microtubule construct will be negatively affected in the protein-rich samples. A previous study by Korten *et al* observed the effect cell lysates; blood serum and plasma; and buffer solutions conducive to PCR and labeling techniques had on cytoskeletal transport systems.[118] The motivation for their work was to establish a kinesin-based platform for personalized genomic diagnostic applications. In this Korten *et al* study the kinesin-MT system was found to be compatible with blood plasma and blood serum when blood derivatives made up 0.1% of the buffer solution; with cell lysates that contained 5000 cells μl^{-1}; and a variety of buffer solutions and were not compatible in DNA hybridization conditions.

The array of proteins signaling the presence, progression, or regression of diseases is unique to each individual disease. The protein landscape required of various diagnostics is diverse and varies in complexity (number of analytes required for proper diagnosis), sensitivity (detection or concentration limits required), and temporally (protein landscape may change at various stages of the

disease). And, the protein landscape of each disease is unique in each type of bodily fluid used for the diagnosis. Today, blood serum and plasma are the most common samples used in proteomic ELISA assays because of they tend to contain relatively high concentrations of proteins present, which is desirable as it makes the assay more robust. However, all of the other aforementioned biological samples have distinct benefits that are driving the development of new diagnostic test platforms.

Reflecting back on the four facets driving diagnostic technologies (lower detection limits, faster assays, more accurate tests limiting error, and reducing the costs and invasiveness of tests), protein concentrations affecting detection limits and the method of obtaining the biological sample affecting the physical invasiveness of the test are the two facets that are governed by the sample as opposed to the engineering of the diagnostic device. While blood contain high concentrations of proteins, it is invasive to collect the sample from the patient because it require breaking the patients skin, similar to CSF. Furthermore, the more invasive samples require skilled technicians, sterilized equipment, and can only be taken in limited amounts so as not to negatively affect the patient. The invasiveness of these protein-rich samples is a major limiting factor in many diagnostic tests in resource-limited environments. Relying on non-invasive samples such as saliva and urine is more desirable as they are less expensive, available in large volumes without affecting the patients' well being, and eliminate the risk of infection or agitation to the patient. However, the trade off associated with these non-invasive samples is that common protein biomarkers are generally found in lower amounts if they are even present at all. As mentioned in the prior discussion on proteomic biosensors, advances in

engineering and scaling down diagnostic tests is lending the field to more robustly being able to detect lower concentrations of proteins for disease detection. These engineering advances are, therefore, encouraging the development of new diagnostic standards and arrays to be investigated and implemented into diagnostic devices using noninvasive samples that I will further explore in this dissertation.

CHAPTER 3

ANTIBODY-FUNCTIONALIZED NANOSHUTTLES DRIVEN BY BIOMOLECULAR MOTORS FOR SENSITIVE IMMUNOASSAY APPLICATIONS

In this chapter I discuss the progress I made in further advancing and characterizing antibody functionalized microtubules that can be used for sensitive immunoassay applications. I developed a covalent conjugation technique that uses a heterobifunctional crosslinker to specifically attach antibodies to microtubules resulting in antibody-functionalized nanoshuttles for innovative immunoassay platforms. This technique is effective for a variety of antibody types, is highly specific, binds high densities of antibody (>100 antibodies μm^{-1} of microtubule), and does not sacrifice the active transport properties of microtubules and their kinesin motor counterparts. The conjugation design allows antibody-functionalized microtubules and antigen to diffuse freely in solution, which significantly reduces typical enzyme-linked immunosorbent assay (ELISA) times. The nanoshuttles can be concentrated to yield very high antibody to antigen ratios ideal for ultralow antigen detection or to remove undesired proteins or dyes from solution. Intrinsic motility characteristics of the complementary biomolecular kinesin motors can be incorporated into advanced actuation or concentration mechanisms in micro- or nanofluidic devices ideal for novel immunoassay platforms.

3.1 Introduction

In clinical settings detecting low levels of protein via immunoassays that leverage high affinity antibodies is critical for early disease detection. In the past decade the miniaturization of immunoassay platforms and a variety of microfluidics-based lab on a chip (LOC) designs have been a major driving force in a steady progression towards lower detection limits, reduced assay times, and less invasive procedures.[119, 120] One strategy is to harness the MT-kinesin transport system as microshuttles for nano biotechnology applications, as justified in Chapter 2. This approach led several groups to functionalize microtubules with antibodies with the intent to transport specific target protein cargos in LOC systems.[24, 32, 33, 41, 42, 45, 46] While data from this work support this general concept, existing protocols broadly suffer from a range of limitations. First, functionalized MTs should ideally be able to freely diffuse within the sample without creating crosslinking byproducts such as MT and antibody aggregates. Freely diffusing MTs significantly reduce incubation times, reduce the complexity of handling procedures, prevent MT aggregates from forming that hinder *in vitro* motility, and reduce the unnecessary waste of expensive reagents. Crosslinking was most prevalent in conjugation techniques that relied on multivalent streptavidin-biotin linkages or homobifunctional crosslinkers. Second, conjugation methods should be applicable to a wide variety of commercially available antibodies including antibody fragments and recombinant antibodies. Third, the binding capacity, meaning the number of functional antibody molecules per length of MT, needs to be high to realize

assays capable of detecting femto- to nanomolar protein concentrations. To develop sensitive and robust immunoassays, it is therefore essential that this metric be quantified to evaluate the potential of functionalized MTs for immunoassay platforms. Additionally, antibody-functionalized microtubules must retain their motile properties with biomolecular motors.

To achieve my goal of realizing antibody-functionalized microtubules with the full complement of properties desired for advanced immunoassay applications, I developed and quantitatively characterized a covalent conjugation technique that utilizes a heterobifunctional crosslinker to specifically conjugate antibodies to microtubules. This technique prevents undesired crosslinking byproducts, is effective for monoclonal, polyclonal, recombinant, and $f(Ab)'_2$ antibodies, is highly specific, binds high densities of antigen and does not sacrifice the motility properties of the MT-kinesin system.

3.2 Approach

The basic approach to our method is outlined in **Figure 3.1**. A free amine on the polymerized MT surface and a reduced sulfhydryl group on the antibody heavy chain are covalently linked via the heterobifunctional succinimidyl 4-(N-maleimidomethyl)cyclohexane-1-carboxylate (SMCC) crosslinker (Pierce 22360). SMCC is 8.3 Å long and contains an amine-reactive succinimidyl (NHS) ester moiety on one end and a sulfhydryl-reactive maleimide moiety on the other. The sulfhydryl group on the antibody intended for modification is an attractive target because it neither sterically nor chemically interferes with the antigen-binding domain, which is ideal for a successful immunoassay platform.

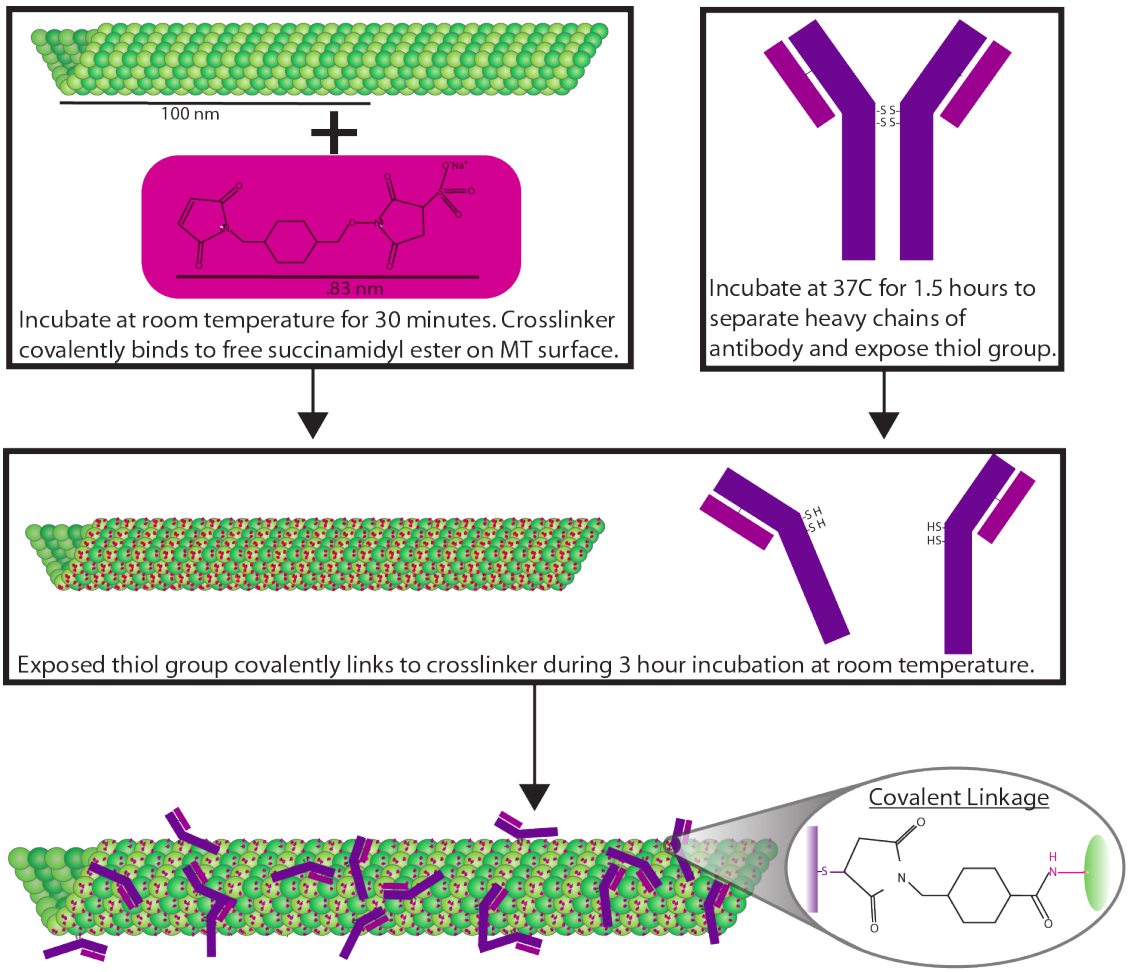

Figure 3.1 Conjugation protocol. Microtubules functionalized with the heterobifunctional SMCC crosslinker. Monoclonal, polyclonal, or f(Ab)'$_2$ antibodies were reduced, and the exposed disulfide bond on the antibody heavy chain was covalently bound to the SMCC-coated MT surface.

The labeling procedure begins by activating MTs with an excess of SMCC crosslinker. The amine-reactive NHS ester reactions were continued for 30 minutes at room temperature to allow sufficient crosslinker binding to the MTs. Detailed characterizations of SMCC-labeled MTs (MT-SMCC) via Ellman's Assays also showed that the hydrolysis of the maleimide moiety of SMCC to maleamic acids was sufficiently slow (see **Experimental Section**) such that the reactivity for binding antibodies is preserved under these labeling conditions.[121]

After the MT-SMCC conjugation, excess SMCC was removed from solution to promote antibodies binding to MT-SMCC and avoid antibodies binding to crosslinker free in solution. To remove free SMCC from solution, MT-SMCC were spun in an ultracentrifuge (Beckman Airfuge) for 30 seconds at 30 psi through a 60% glycerol cushion containing 20 μM paclitaxel (LC Laboratories P9600) and resuspended in a sodium phosphate buffer with 20 μM paclitaxel. The disulfide bonds linking the antibody heavy chains were reduced in a 50 mM 2-Mercaptoethylamine (2-MEA) solution for 90 minutes at 37° C to separate the two heavy chains. To prevent any further reduction of antibody, excess 2-MEA was removed through a buffer exchange column.[122, 123] This also avoids interference with maleimide-sulfhydryl binding. Reduced antibodies were immediately added to MT-SMCC at a 2-, 6-, or 10-fold molar excess with respect to the total tubulin concentration, and the solution incubated for 2.5 hours at room temperature to complete the conjugation. Then, free antibodies were removed by pelleting the antibody-functionalized MTs via centrifugation and resuspending them in 80 mM PIPES buffer containing 20 μM paclitaxel.

3.3 Results

Specificity and Binding Capacity of Antibody-Functionalized Microtubules

To characterize the specificity and binding density of antigen on the functionalized MTs, I performed binding assays as illustrated in **Figure 3.2** using microtubules functionalized with polyclonal anti-bovine serum albumin (anti-BSA) (Molecular Probes, A11133), pepsin digested $f(Ab)'_2$ anti-BSA, or monoclonal anti-human interleukin 6 (anti-IL-6) antibodies (Invitrogen,

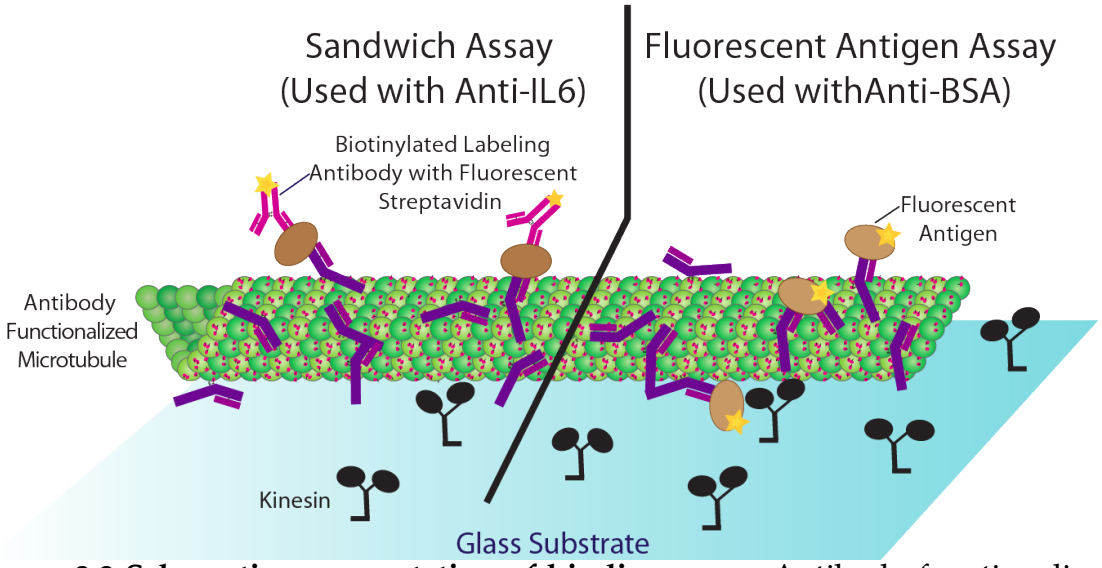

Figure 3.2 Schematic representation of binding assay. Antibody-functionalized microtubules are labeled with either fluorescently tagged labeling antibody (left) or a fluorescently tagged antigen (right) in binding assays. The kinesin-coated glass substrate also supports gliding motility when ATP is available in solution.

CHC1263). The assays were carried out in simple microfluidic chambers constructed form microscope slides and coverglasses. First, I sequentially coated the chambers with buffer solutions containing casein and kinesin that adsorbed to the glass surfaces. This reduces nonspecific binding of free antigens or fluorophores to the glass surface during the assays. In addition, when MTs were introduced in the microfluidic chambers, they bound to kinesin motors (specifically the N-terminal motor domains) attached to the glass surface. Consequently, the microtubules were held nanometers from the glass surface for imaging. When ATP was present in the assay buffer, MTs were transported along the kinesin-coated surface in *in vitro* gliding assays. Tetramethylrhodamine (TMR)-labeled BSA served as the anti-BSA antigen while unlabeled IL-6 in combination with an anti-IL6 biotinylated detection antibody labeled with TMR streptavidin was used to detect anti-IL6 on the MT surface. To qualitatively

analyze how antibody-functionalized MTs capture their respective antigens, I polymerized fluorescently-labeled microtubules by incorporating a small fraction of Cy5-labeled tubulin, functionalized the microtubules with antibodies using our SMCC crosslinking protocol and then used fluorescence microscopy to separately image microtubules and complementary as well as non-complementary antigens. As illustrated in **Figure 3.3**a, antigen molecules bound to MTs functionalized with complementary antibodies but not to MTs with non-complementary antibodies or unlabeled microtubules. For example, as shown in the third column of **Figure 3.3**a, TMR-BSA bound only to anti-BSA functionalized MTs while untreated and anti-IL-6 functionalized MTs showed negligible rhodamine fluorescence signals in the presence of even very high concentrations of TMR-BSA (100 nM). Similarly, the binding behavior of IL-6 (second column) shows interactions with complementary anti-IL-6 functionalized MTs while untreated MTs and anti-BSA functionalized MTs did not bind IL-6. I also note fluorescent specks in the images not associated with MTs, particularly in the complementary antigen TMR images. Based on a number of control experiments, I believe that these specks represent labeled, functionalized MT fragments that invariably result from the handling procedures associated with pelleting and resuspending MTs. Note however, that these specks do not represent background nor nonspecific labeling associated with the functionalized MTs. All of the IL-6 images were taken using TIRF microscopy at higher magnification (note the longer scale bars). IL-6 assays had lower signal to noise ratios and, therefore, inherently highlight the residual fluorophore on the glass surface, which is an artifact of incomplete protein blocking. Taken together, these observations suggest that the binding of antigen to functionalized MTs is

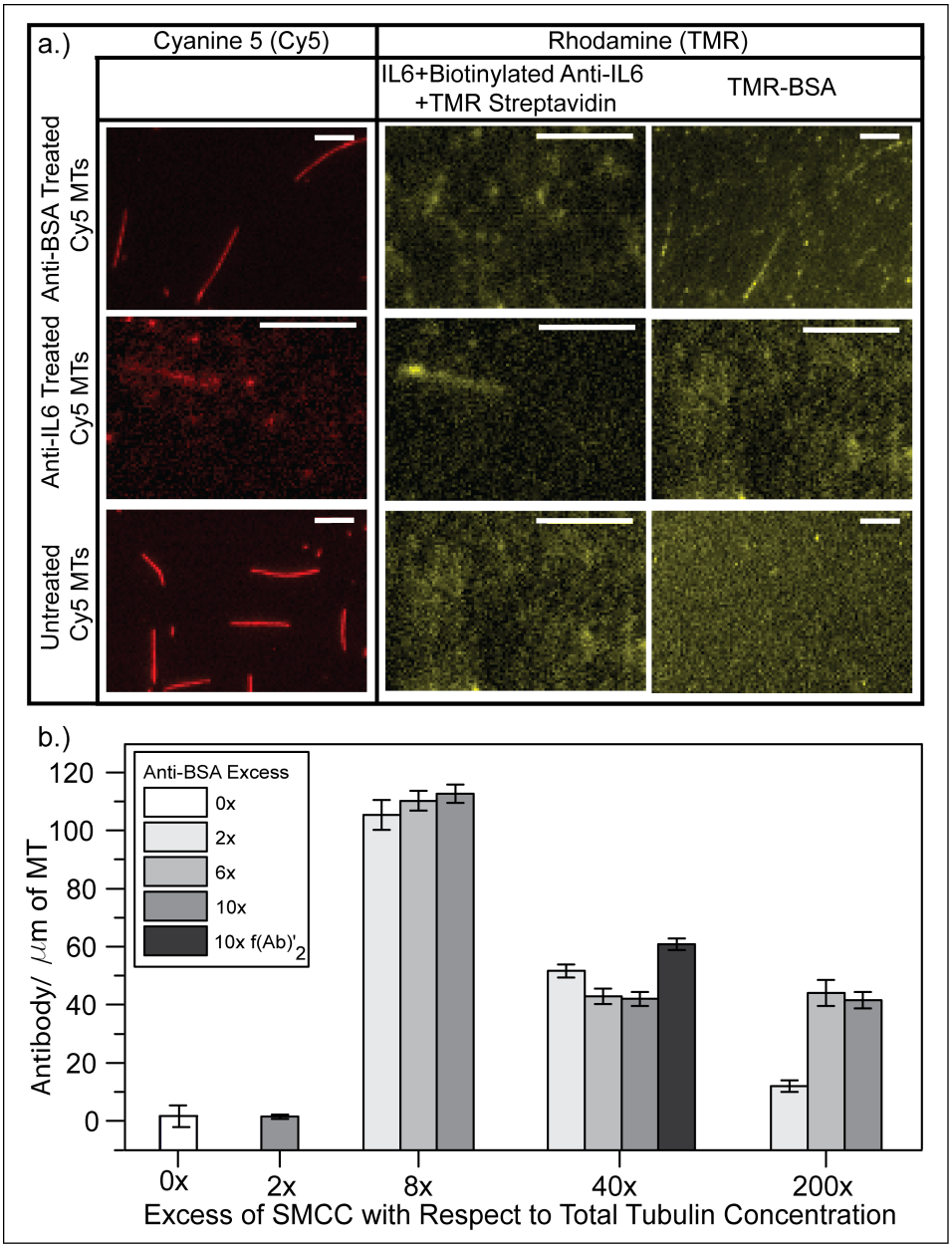

Figure 3.3 Antigen specific binding and binding capacity. a.) Cy5 microtubules were either treated with polyclonal anti-BSA IgG (top row), monoclonal anti-IL6 (middle row), or not treated (bottom row) and incubated with 100 nM TMR-BSA (right column) or 100 nM IL-6 and TMR labeled detection antibody (middle column). Antigen binding is specific to treated, antibody-functionalized microtubules. Labeling IL-6 with a fluorescently-tagged detection antibody resulted in higher background noise that required TIRF microscopy. **b.)** TMR-labeled microtubules functionalized with Anti-BSA IgG and incubated in 100 nM TMR-BSA solution. The intensity of the fluorescent signal correlates with the fluorescent antigen bound, which is plotted with respect to the conjugation conditions. The error bar represents the standard error of each measurement ($30 < N < 80$).

specific and the antigenicity of our functionalized MTs, a fundamental requirement for future immunoassay applications, is preserved.

In the context of the envisioned applications, it is important to characterize the specificity of antigen binding to determine if nonspecific binding of antigen to the MT surface will limit antigen detection and ensure that our results are applicable to a wide range of antigens. Ideally, nonspecific binding would be sufficiently low (characterized by a dissociation constant K_D that is significantly higher than that of the antibody) such that the specificity (defined by the ratio of antigen molecules bound to antibody on the functionalized MT to the number nonspecifically adsorbed to the MT surface) would not limit the resolution of the assay. To quantitatively measure binding of fluorescent analyte to MTs, I quantified the fluorescence intensities from MT surfaces and relate these to calibrated intensities (See **Figure 3.4**). I measured the amount of TMR-BSA that binds to untreated MTs, which is representative of the nonspecific binding of antigen to functionalized MT surfaces. Specifically, I incubated untreated MTs with 100 nM, and 1 μM TMR-labeled antigen for 30 minutes and then measured the number of rhodamine dye molecules on the MT surface. Nonspecific binding was negligible at 100 nM with only 1.7 ± 3.7 BSA μm^{-1} (N=27) adsorbing to the MT surface. Nonspecific BSA binding became significant only at 1 μM TMR-BSA in solution where unfunctionalized MTs bound 33.8 ± 5.4 BSA μm^{-1} (N=49) of MT. The observed adsorption behavior results in a nonspecific dissociation constant several orders of magnitude higher than the dissociation constant for a typical antibody (10^{-10} M) and is consistent with low-affinity, nonspecific protein- protein interactions as observed by others.[124] Since

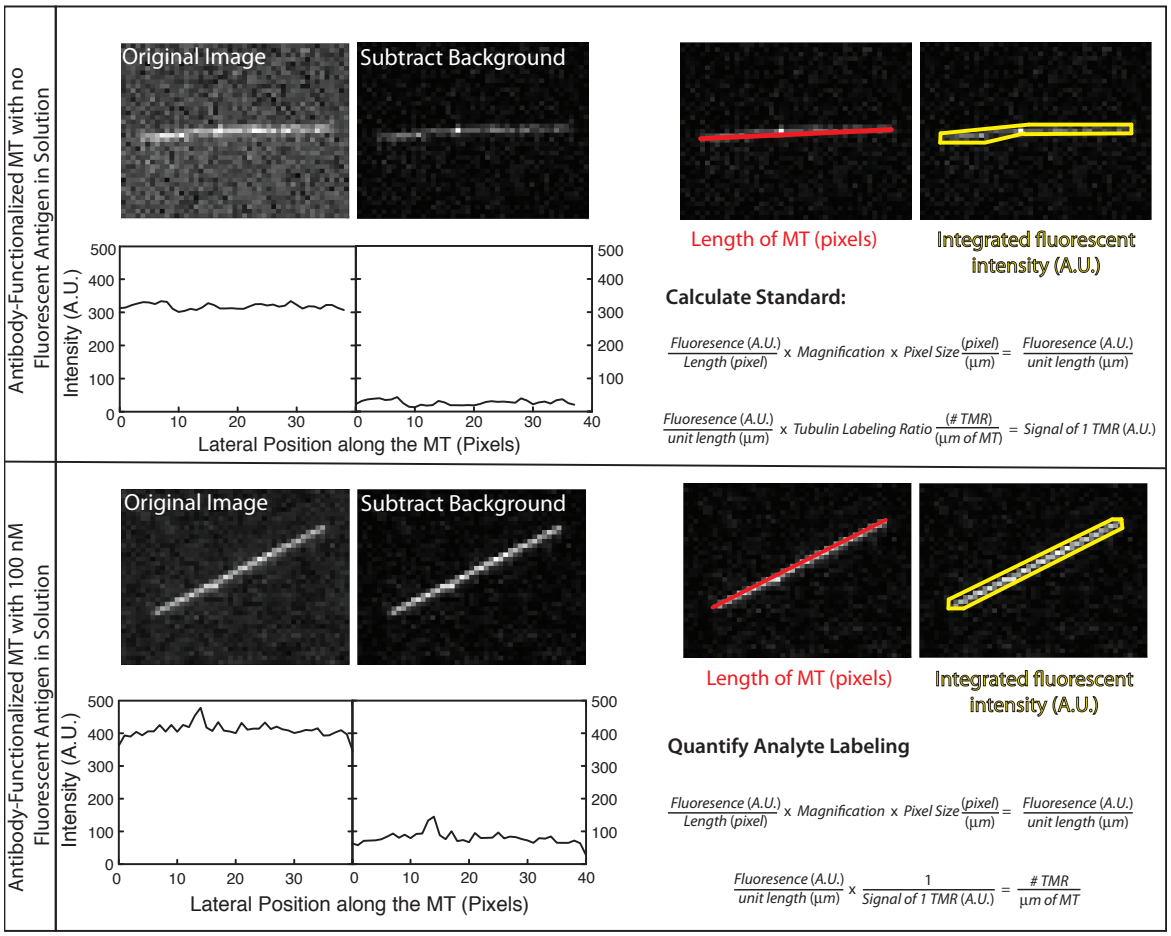

Figure 3.4 Image processing for binding capacity measurements. First, the background was subtracted (*left*). The length and integrated fluorescent intensity of MTs labeled with rhodamine at a known labeling ratio were measured to determine the standard fluorescence for a single rhodamine dye (*top right*). The same length and fluorescence measurements were done on functionalized MTs under the same imaging conditions. From here, I calculated the number of rhodamine-labeled antigens on a MT (*bottom right*).

the ratio of nonspecific to specific analyte binding is <10%in the presence of 100 nM antigen for anti-BSA and f(Ab)'$_2$ anti-BSA, I can conclude that antigen binding is highly specific, and integrating kinesin and microtubules into this immunoassay platform does not sacrifice nor interfere with the specificity of antibody-antigen binding.

To predict the potential these engineered nanoshuttles have in future immunoassay applications, I characterized the binding capacity of these functionalized MTs. I define the MT binding capacity as the number of antigen molecules a MT carries per unit length when all antigen-binding sites on the MT are theoretically occupied. To determine the binding capacity, I refer to ligand-receptor kinetics to ensure that an antigen occupies every antibody in our binding capacity assays. The dissociation constant of a typical antibody is $K_D = \frac{k_{off}}{k_{on}} \approx 100\,pM$, where $k_{on} \approx 10^6\,M^{-1}\,sec^{-1}$ and $k_{off} \approx 10^{-4}\,sec^{-1}$.[125] If I define R as the concentration of antibody (receptor) in solution, L as the concentration of antigen (ligand) in solution, then C, the concentration of bound antibody-antigen, is given by

$$R + L \rightleftarrows_{koff}^{kon} C$$

and the kinetics of our system is

$$\frac{dC}{dt} = k_{on}RL - k_{off}C.$$

At equilibrium ($\frac{dC}{dt} = 0$), neglecting the effect of ligand depletion and assuming this limit is asymptotically approached for $t \gg (k_{on}L_{total} + k_{off})^{-1}$, then

$$C_{equilibrium} = \frac{R_{total}L_{total}}{K_D + L_{total}}.$$

Binding capacity assays were done with 100 nM antigen and < 0.2 nM antibody bound to microtubules in solution. Thus, the conditions of the binding capacity assays are conducive to 99.9% of antigen binding sites being occupied after a 25-minute incubation according to the assumptions stated above.

Using workable concentrations of crosslinker and anti-BSA antibody, I varied the concentrations of SMCC and antibody to maximize the binding

density of the conjugation. Binding capacity assays were performed using the same protocol used for specificity assays. I achieved a maximum binding capacity of 112.6 ± 3.2 antigen molecules per micrometer of microtubule as shown in **Figure 3.4**b. Our data illustrate that optimal, high binding capacities depend mostly on using the appropriate excesses of SMCC in the conjugation. High excesses (40- and 200-fold excesses of SMCC with respect to total tubulin) result in fewer antigens bound to the functionalized MT. At low crosslinker concentrations (2-fold excess) I consistently observe low antigen densities on the microtubules (1.5 ± 0.72 BSA μm^{-1} (N=83)), resulting in optimal labeling at approximately 8-fold SMCC excess. I also conducted additional measurements (data not shown) at intermediate SMCC stoichiometries (10- and 14-fold) that showed that the optimum crosslinker concentration for our experimental conditions is close to an 8-fold excess, and the antibody density as measured by the number of functional antibodies per unit length of microtubule declines monotonically from this optimum. I believe that this optimum is the result of two of competing mechanisms. At SMCC concentrations below the optimal 8-fold excess, the number of tubulin dimers labeled by the amine-reactive group in the crosslinker is limited, and consequently, increasing SMCC concentrations led to more antibody binding. On the other hand, while high concentrations of SMCC activate nearly all tubulin dimers, excess SMCC at increasing stoichiometries are practically impossible to completely remove from the MT preparation, and unbound reagent in solution reacts quickly with antibodies such that the number of antibodies binding to the MT is reduced. While I do see a strong correlation between SMCC concentration and binding capacity, the correlation between

antibody excesses and binding capacity is not apparent for the range of antibody excesses used here. In addition to attaining high binding densities on the MT shuttles, another important consideration is that the motility properties of the MT-kinesin system remain intact after functionalization and analyte capture.

Motility Properties of Antibody-Functionalized Microshuttles

Since the kinesin-MT interactions depend on electrostatic and steric interactions to sustain motility, there are concerns that heavily functionalizing a MT can prevent or impair kinesin motility.[32] To characterize the effect our conjugation method has on the motile properties of the kinesin-MT system, I measured the speed using gliding assays in the presence of 10 nM analyte (see **Experimental Section**) (**Figure 3.5**). The kymograph shown in **Figure 3.5**a shows that the quality of gliding assay motility with antibody-functionalized MTs is similar to unfunctionalized MTs. Looking at the white columns in **Figure 3.5**b where no antibody is on the MT, I conclude that SMCC excesses have a slightly negative effect on gliding assay speeds. I do not see a consistent correlation between antibody excesses and gliding assay speed. Steric issues that would likely be caused by the large antibody are not a problem as I see only a 33% velocity decrease down to 800 nm sec^{-1} when the MT contains over 100 antibodies μm^{-1} in the 8-fold SMCC 10-fold antibody assay. The SMCC crosslinker appears to be sufficiently small as to not terminate motility. Kinesins seem to easily accommodate for antibodies, which label only 5-10% of tubulin dimers. The conjugation parameters I tested using anti-BSA and TMR-BSA revealed a range of conditions where the effects on motility are moderate, and the functionalized

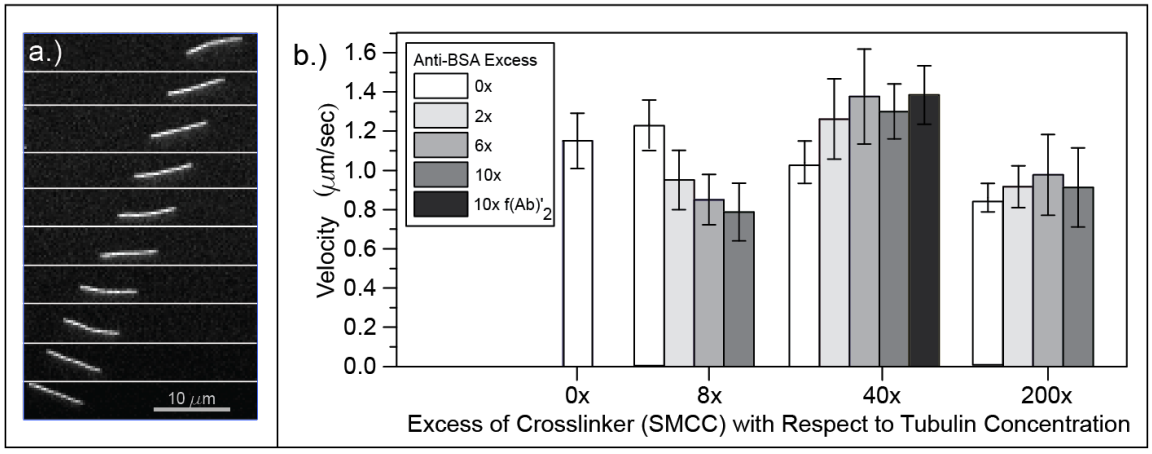

Figure 3.5 Functionalized microtubules support motility. a.) Kymograph of a microtubule functionalized with anti-BSA in 10 nM TMR-BSA demonstrating that kinesin motility is largely unaffected under the conditions used. Frames are separated by 2 seconds. b.) Velocity of anti-BSA functionalized microtubules in 10 nM TMR-BSA solution was measured in gliding assays. The error bar represents the standard deviation of each measurement.

MTs are capable of supporting robust gliding assays that can be integrated into an active transport system.

Limitations for Sandwich Assay Construct

Ideally, for diagnostic applications one would prefer to utilize an antibody sandwich assay construct that takes advantage of a labeled complementary antibody to detect the analyte (See **Figure 2.3**). Labeling with a second antibody is more advantageous than the detection method used in the anti-BSA results discussed above because the analyte itself does not need to be directly labeled for detection. Directly labeling the analyte specifically without the use of a labeled detection antibody is unrealistic for diagnostic applications. Covalent labeling proteins relies on generic labeling chemistries that target specific moieties but are unable to distinguish between the same moieties on two different proteins.

Therefore, to specifically covalently label protein analytes, the analyte must be purified from the sample using various chromatography and/or filtration techniques and then labeled using these generic labeling chemistries. Purifying the sample to specifically label the analyte is necessary to maintain low background fluorescence and to eliminate false signals caused by cross-reactive species. The yield of such a purification and labeling procedure is generally low (<20%), and furthermore, once the protein analyte is purified from the sample to be labeled, such an ELISA platform is unnecessary since protein concentrations could be determined using other techniques such as absorbance measurements. Therefore, using fluorescently tagged secondary or complimentary antibodies for analyte detection is the ideal method for detecting protein analytes in ELISA assays.

My results indicate that there are limitations in incorporating antibody sandwich assays into this microtubule-based immunoassay platform with regards to motility. Sandwich assays were used to confirm that IL-6 cytokine binds to anti-IL-6 functionalized microtubules as see in **Figure 3.3**a. **Figure 3.6** shows how gliding assay motility is affected as the antibody sandwich is assembled for IL-6 detection. As discussed in detail previously and illustrated in **Figure 3.5**, covalently binding the primary antibody and BSA antigen to the microtubule surface does not significantly impair gliding assay motility. However, attaching a detection antibody significantly affects motility by reducing gliding velocity over 3-fold to <500 nm sec^{-1} and leading to poor quality motility.

Three parameters were measured to characterize quality of motility. A microtubule with poor quality motility is either tethered to the kinesin-coated surface or has a 'floating end.' Tethered microtubules are not motile, have zero velocity, and were not included in velocity measurements. Oftentimes, tethered microtubules appear to be twitching on the surface, suggesting that motors are making contact with the microtubule but an additional mechanism is preventing the microtubule from being propelled forward by the motor. Microtubules with floating ends are motile, but one of the microtubule ends is freely diffusing in solution while the rest of the microtubule is bound to the kinesin-coated surface, which propels it forward (See **Figure 4.4**). Floating ends contribute to poor quality motility because these free ends can lead to the microtubule dissociating from the kinesin-coated surface over time. As the quality of motility is reduced as the antibody sandwich is assembled, there is also a significant drop in the number of events per field of view. **Figure 3.6** shows that the percent of motile microtubules and their velocities are positively correlated. The percent of microtubules with poor quality motility are negatively correlated to the change in velocity and percent of microtubules that are motile. In this case, reducing microtubule gliding velocity is indicative of the quality of motility deteriorating.

To determine if the mechanism driving the degradation of motility with the sandwich assay construct is steric, additional experiments were done. Constructing the full sandwich assay requires several additional flow and rinse steps through the assay chamber (See **Experimental Section**). Using the same anti-IL-6 functionalized microtubules with no antigen or secondary antibody, flowing through an equivalent amount of motility buffer at the same time points

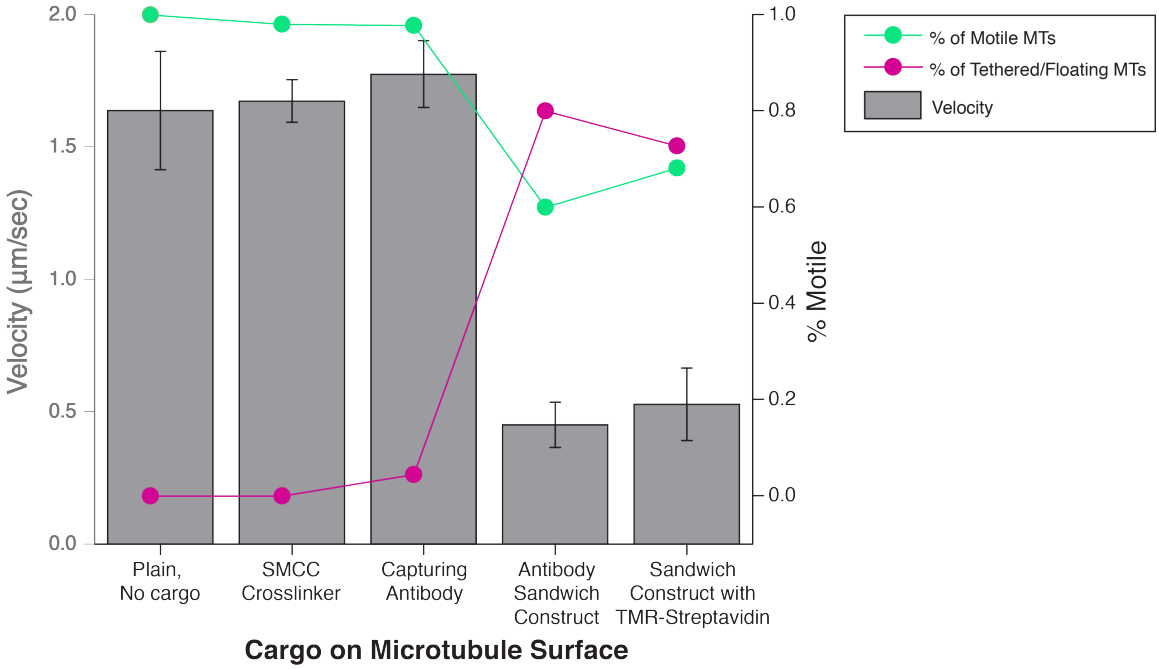

Figure 3.6 Effect of antibody sandwich cargo on kinesin-microtubule gliding assay. The velocities at various stages of anti-IL-6 labeling were measured. The gliding velocities of microtubules carrying antibodies and antigens are not negatively affected. However, once a detection antibody binds to the antigen complex, the velocities and quality of motility are severely affected. Error bars show standard deviations.

did not decrease the velocity or quality of motility. These results demonstrate that the additional time and flow steps used in these experiments do not negatively impact the kinesin-coated surface. To ensure that neither the secondary antibody nor the TMR-STV has an effect on motility, unfunctionalized microtubules were used in the same assay where they incubated with the anti-IL-6 secondary antibody and then TMR-STV. Neither velocity nor motility quality changed in these assays. Based on these results, I conclude that the negative impact on gliding assay motility is not caused by the assay itself but is, instead, likely caused by steric hindrances brought about by the large sandwich assay construct on the microtubule surface. The bulky construct appears to create

microtubules that become tethered on the surface. These observations suggest that the antibody sandwich construct cannot be effectively incorporated into the aforementioned microtubule concentrator device with the current assay conditions. The low microtubule densities and inability for these microtubules to move processively for long periods of time (50 minutes) prevent a sufficient number of microtubules from concentrating to make significant observations. The limitations and potential for antibody sandwich assay constructs in kinesin-driven technologies are further discussed in Chapter 5.

3.4 Conclusions

The overall goal of this work was to functionalize microtubules with antibodies such that they can serve as both an immunoassay substrate and a micro-transport mechanism that can bind low concentrations of antigens in solution. Our results illustrate that the functionalization method presented here specifically binds complimentary antigen from solution and maintains motility. An additional advantage is that this method is well suited for a wide variety of commercially available antibodies including monoclonal, polyclonal, and $f(Ab)'_2$, and it is also compatible with recombinant antibodies. Based on the coupling chemistry and the high binding capacity, the technique described in this paper is well suited for detecting low concentrations of antigen if directly integrated into a microtubule concentrator device such as that developed by Lin *et al*.[80] Using realistic antibody densities established in this work and the device geometry reported in our previous work, I estimate that in a 10 nL sample, a total length of 5 mm of functionalized MTs holding ~100 antibodies μm^{-1} could capture all of

the six antigen molecules found in a 1 fM antigen solution after a 25 minute incubation assuming that the antibody-antigen complex has a dissociation constant (K_D) ≤ 100 pM and the only antibodies in the system are those on the MT surface.[80] I believe that the functionalization method developed here holds significant potential for sensitive immunoassay applications. By leveraging short assay times, sensitivity, the ability to concentrate antigen to lower background noise, and retaining antigenicity, these results suggest that the characteristics of our functionalized MTs are well suited for advanced, microfluidic immunoassay or protein delivery platforms. The next step is to integrate these antibody-functionalized MTs into an immunoassay platform to extract and detect specific proteins from medically relevant samples.

3.5 Experimental Section

Microtubule Preparation

Tubulin was extracted from bovine brain using a high salt cycling purification protocol and alternate polymerization and depolymerization cycles.[126] Microtubules for functionalization and motility assay were polymerized in a solution containing 2.0 mg ml^{-1} tubulin, 4.0 mM $MgCl_2$, 1.0 mM GTP, and 5% DMSO in BRB80 buffer (80 mM K-PIPES, 1.0 mM EGTA, 1.0 mM $MgCl_2$; pH 6.8). The polymerization solutions were incubated at 37° C for 30 minutes and then stabilized by diluting the solution 4-fold in a BRB80 and 20 μM paclitaxel (LC Laboratories P-9600) solution. Labeled tubulin dimers were labeled with amine reactive dyes 5-(and-6)-carboxythetramethylrhodamine (Molecular Probes C1171) or cyanine-5 (GE Healthcare, PA15104). Excess dye

was quenched with K-glutamate, and microtubules were removed from the dye through polymerization and cycling. Labeling ratios of dye to tubulin was determined by absorbance measurements (Shimadzu BioSpec) and the Beer-Lambert law.

Kinesin Purification

A kinesin motor consisting of the head and neck domain of *Neurospara crassa* kinesin (amino acids 1-433) and the stalk of *Homo sapiens* kinesin (amino acids 433-560) with a cysteine tag called NKHK560cys was used. Motors were expressed and purified as described by Lakamper, *et al*.[127] Briefly, motors were expressed in DH5α *Escherichia coli* cells and purified using cation exchange chromatography (GE 17-5054-01).

Microtubule Antibody Conjugation

The following buffers were degassed using a vacuum pump and flushed with dry nitrogen gas before the conjugation procedure: PBS (100 mM Sodium Phosphate, 0.15 M NaCl; pH 7.2), Activation Buffer (100 mM Sodium Phosphate, 0.15 M NaCl, 10 mM EDTA; pH 7.2), Cushion (0.1M NaHEPES, 1.0 mM $MgCl_2$, 1.0 mM EGTA, 60% v/v glycerol; pH 6.8). Microtubules were polymerized, spun down, and resuspended in PBS containing 20μM paclitaxel (+T). SMCC crosslinker was dissolved in DMSO at 4 mg ml^{-1}, added to microtubules at the desired molar excess, and incubated at room temperature for 30 minutes. Excess crosslinker was removed from solution by spinning the treated microtubules through the cushion +T. SMCC treated microtubules were resuspended in

activation buffer +T. Antibodies were reduced in 50 mM 2-Mercaptoethylamine (Thermo 20408) in activation buffer for 90 minutes at 37° C. 2-MEA was removed from the buffer through buffer exchange columns flushed with nitrogen. Reduced antibodies were immediately added to SMCC-MTs at the desired molar excess. $F(Ab)'_2$ fragments underwent a pepsin protease digestion (Pierce, 44688) and were frozen before used in the assay. Antibodies and microtubules incubated at room temperature for 2.5 hours in a nitrogen flushed environment. Excess antibody was removed by spinning and pelleting antibody functionalized MTs, removing the supernatant containing free antibodies, rinsing the pellet, and then resuspending the functionalized MTs in BRB80 +T.

Ellman's Reagent Assays

Ellman's reagent (Pierce 22582) is a solution that drives a color change when it interacts with free maleimide moieties. Dissolve Ellman's reagent at 4 mg ml^{-1} in Activation Buffer (see above). Prepare samples such that you expect to have 0.1-1.0 nmoles of maleimide in solution. Samples should include the crosslinker or protein of interest and contain sequential dilutions of cysteine (0.0~5.0 nmoles). A standard curve should be done in parallel containing only cysteine dilutions. Add 20 µL Ellman's solution to 100 µL sample and 1 mL degassed Activation Buffer flushed with nitrogen. Measure the absorbance of the solution with excitation at 412 nm in the spectrophotometer. Plot the absorbance measurements such that the number of moles of cysteine is on the x-axis and the absorbance measurement is plotted on the y-axis. The control curve should be a straight line with a constant slope, *m*. The maleimide-containing sample of interest will contain a horizontal lag that signifies

free maleimide in solution. The point at which the horizontal lag ends and the a straight line with slope *m* continues correlates to the amount (moles) of reactive maleimide in solution.

Binding Capacity Assays

Antibody-functionalized microtubules were allowed to freely diffuse in solution with 100 nM analyte unless otherwise stated for 25 minutes. First, a precoat of 0.1 mg ml^{-1} casein in BRB80 was flown through the microfluidic chamber and allowed to incubate for 3 minutes. Subsequently, a kinesin solution containing 0.05 mg ml^{-1} casein and 0.12 mg ml^{-1} NKHK560cys in BRB80 +T was introduced into the chamber and incubated for 5 minutes. Then, antibody-functionalized MTs and analyte were added to the chamber and allowed to incubated for 5 minutes followed by a BRB80 +T rinse set consisting of at least 8 chamber volumes to rinse away free analyte. For IL-6 assays, the labeling antibody was flown through and incubated for 1 hour. After washing the chamber, rhodamine-labeled streptavidin was flown through in excess and is immediately rinsed with five chamber volumes of BRB80 + T. Samples were visualized in epifluorescence using a Zeiss Axiovert 200 microscope and Zeiss Plan-Neofluar 40x/1.3 oil immersion objective illuminated by a mercury arc lamp unless otherwise noted. Image sequences were recorded with a Hammamatsu ORCA ER series camera. Quantitative analysis was performed using ImageJ software.

Motility Assays

The assay begins with the same surface precoating and kinesin incubation sets described for the binding capacity protocol. Motility buffer (2 mM $MgCl_2$, 0.05 mg ml^{-1} casein, 0.08 mg ml^{-1} catalase, 0.1 mg ml^{-1} glucose oxidase, 10 mM glucose, 10 mM DTT, 1mM ATP) containing 10 nM analyte and functionalized MTs were incubate for 20 minutes and then flown through the chamber. The chamber was sealed and microtubules incubate for 5 minutes before visualization.

CHAPTER 4

KINESIN AND MICROTUBULE COMPATABILITY IN HUMAN URINE, SALIVA, AND BLOOD PLASMA

Chapter 3 demonstrated that microtubules can be transformed into microshuttles to transport specific protein cargos. These findings show that functionalized microtubules can serve as useful platforms for advanced immunoassay applications. To further advance the kinesin-microtubule system in medical diagnostic platforms, one major gap of knowledge in the field must be addressed. Understanding how medically relevant samples affect the kinesin-microtubule system is critical in moving this active transport system into applied technologies. In this chapter I will assess the compatibility of the kinesin-microtubule system in human urine, saliva, and blood plasma. The potential of this system in complex, protein rich body fluids will be characterized by its ability to bind cargos and move in gliding assays. Conclusions and discussions will be framed to relate our results to the current transport requirements kinesin-driven technologies have.

4.1 Introduction

Concerns regarding the kinesin and microtubule system's motility properties being compatible with more complex, protein rich body fluids (such

as those listed in **Table 2**) arise because microtubules are not naturally found in body fluids including blood serum, urine, and saliva used in immunoassays. Therefore, these body fluids are not necessarily compatible to kinesin-microtubule functionalities, which brings about two main concerns. First, protein-rich solutions can be detrimental to the nonnative proteins.[128, 129] Incorporating engineered kinesin and chemically stabilized bovine microtubules in mammalian body fluids may bring unforeseen complications. For example, enzymes such as proteases, which are present in blood serum to clot blood and saliva to assist in digestion, can bind and breakdown foreign proteins.[130, 131] Second, as sample solutions become more complex and protein-dense, specific and nonspecific protein-protein interactions occur more frequently. Specific and nonspecific protein interactions can hinder protein function sterically, electrostatically, or conformationally. Because gliding assays rely on kinesin specifically binding to microtubules and microtubule shuttles need cargos to specifically bind to microtubules, steric or electrostatic interferences can be detrimental to the system.

To advance this field in the direction of immuno-based POC diagnostic applications, I pioneered studies with the kinesin-microtubule system in human urine and saliva samples and examined the effects blood plasma has on the kinesin-microtubule system. In the field of POC diagnostic technologies, researchers are honing their efforts to develop diagnostic platforms that rely on urine and saliva samples instead of blood, which is the current standard for most ELISA assays.[93, 94] Consequently, urine and saliva are ideal sample targets for

future diagnostic technologies, which is why they are a focus in this study along with blood plasma.

Here, I will assess the ability for cargos to bind to microtubules in human urine, saliva, and blood plasma. Then, I will look into how these medically relevant samples affect gliding assay motility. Finally, a criterion for assessing the compatibility of gliding assays in blood plasma will be developed by looking at how motility qualitatively changes in blood plasma and how it affects existing kinesin-driven technologies. Further understanding the potential and limitations of body fluids in the kinesin-microtubule system will give engineers the resources to appropriately design next-generation kinesin-driven immunoassay platforms accordingly.

4.2 Biotinylated Microtubules and Their Ability to Bind Streptavidin Cargos in Human Urine, Saliva, and Blood Plasma

The ability for analyte to bind to the surface of functionalized microtubules is critical for microtubules to serve as cargo-carrying microshuttles. As discussed specifically with respect to immunoassay applications in Chapter 3, affecting the quality of antigen binding to the microtubule by reducing the affinity of the antibody, sterically blocking the antigen binding domain, or not having sufficient time for the antigen to bind will negatively impact the antigen capturing capabilities of the system. Therefore, it is important to properly characterize the effect body fluids have on the ability for analyte to bind to functionalized microtubule surfaces to conclude if microtubule-based

microshuttles can be effectively integrated into immuno-based diagnostic platforms.

The affinity of antibody-antigen binding is dependent on a number of factors including pH, ionic strength, and temperature of the sample. While these factors vary across biological samples (See **Table 2**), antibodies can be engineered to be compatible with a variety of samples retain affinities relevant for ELISA applications (10^{-12}-10^{-9} M).[125] The antigenicity of most commercially available antibodies to their antigen are generally considered unaffected by medically relevant samples such as blood, saliva, and urine.[125] One exception would be highly engineered antibodies, typically expressed in bacteria or yeast cultures, with high affinities (10^{-15}-10^{-12} M) that require more controlled and specific buffer conditions to capture very small quantities of antigen.[132] Since standard, commercially available antibodies are typically used in ELISA, I continue this study under the assumption that antibodies themselves are not a limiting factor when microtubules are functionalized as an immunoassay substrate.

To test the effect human urine, saliva, and blood plasma have on the ability of functionalized microtubule to bind cargos, I measured the binding of rhodamine labeled streptavidin binding to biotinylated microtubules in these body fluids and compared the behavior to STV binding to biotinylated MTs in BRB80 buffer. I chose to work with biotinylated MTs instead of antibody functionalized MTs so that I could more comprehensively assess the magnitude of proteins nonspecifically binding to and blocking the microtubule surface. Biotin is very small compared to an antibody (0.24 kDa versus 150 kDa, respectively). Working with a physically smaller receptor protein, I was able to

examine the effects body fluids have on the microtubule surface at a smaller scale. For example, if a cytokine, typically 12 kDa in size, nonspecifically binds to the microtubule surface, it is more likely to sterically hinder a streptavidin from binding to a blocked biotin site that lies very close to the microtubule surface than an antigen from binding to an antibody whose binding site lays several nanometers away from the microtubule surface. Also, since the biotin-streptavidin linkage has been an instrumental method in conjugating various cargos to microtubules (See Chapter 2), characterizing the effect of body fluids on the biotin-streptavidin linkage is also critical in further developing this microtubule-based microshuttle system.

To characterize the ability for the biotinylated microtubule to bind streptavidin, I performed binding assays similar to those carried out in Chapter 3. The assays were done in microfluidic chambers constructed form microscope slides and coverglasses. First, I sequentially coated the chambers with buffer solutions containing biotin-free casein and NKHK560cys kinesin that adsorbed to the glass surfaces. This process was optimized to reduce nonspecific binding of free TMR-streptavidin to the glass surface during the assays. In addition, when MTs were introduced into the microfluidic chambers, they bound to kinesin motors (specifically the N-terminal motor domains) attached to the glass surface, and the microtubules were held nanometers from the glass surface for imaging. Biotinylated MTs were polymerized such that 93% of the tubulin was biotinylated (See **Experimental Section**) and then pelleted in an airfuge at 30 psi for 30 sec and resuspended in buffer containing 20 μM paclitaxel. Spinning down the microtubules removed excess biotin remaining from the labeling procedure

and biotinylated tubulin that was not polymerized. Once the MTs were bound in the microfluidic chamber, the chamber was washed with 5 chamber volumes of buffer to remove any remaining free biotin. Then, TMR-streptavidin dilutions were made in the body fluid being studied with an addition of 20 μM paclitaxel. The streptavidin-containing solution was added to the chamber and incubated for 10 minutes with the biotinylated MTs. Lastly, the chamber was washed at one time with 15 chamber volumes of buffer plus paclitaxel, and the TMR-streptavidin-coated MTs were imaged.

The binding capacities of the biotinylated microtubules were calculated using the same image processing technique discussed in Chapter 3 (See **Figure 3.4**). All of the imaging was done in BRB80 buffer instead of the body fluid of interest. The quantum yield of the dye, which is affected by buffer conditions, was not significantly altered by the exposure to body fluids. Control measurements were done to quantify the effect the binding assay protocol with the three body fluids has on the fluorescence of rhodamine. These results show that the maximum change in fluorescent intensity is 20%, which is within the range of the standard deviation (±10%) for the measurement. The variance of the fluorescent intensity is taken into account in the y-error plotted below in **Figure 4.1**.

Binding assay results are shown in **Figure 4.1**. This data serves as a comparative analysis that illustrates the ability of the microtubule surface to be accessible to and bind medium sized proteins (specifically, the 60 kDa streptavidin). First, in **Figure 4.1**a we confirm that TMR-streptavidin binding is

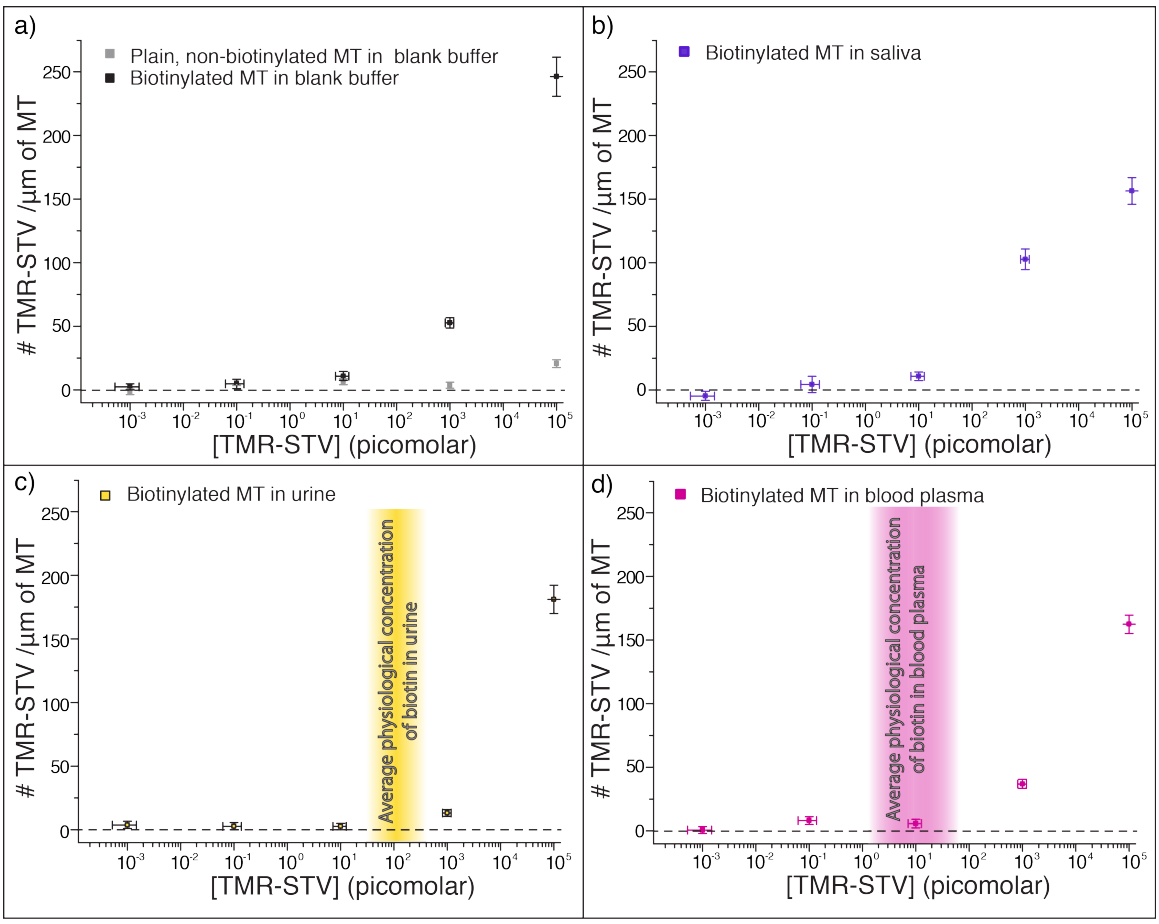

Figure 4.2 Microtubules binding TMR-streptavidin cargos in body fluids. a) TMR-STV binds specifically to biotinylated MTs in buffer. TMR-STV binds to biotinylated microtubules at similar densities while in solutions of 100% b) human saliva, c) human urine, and d) blood plasma.

specific to the biotinylated microtubules. The binding affinity of streptavidin to biotinylated tubulin in BRB80 buffer is at least an order of magnitude larger than streptavidin to unlabeled tubulin. Looking at the 100 nM and 1 nM measurements for all samples tested (See **Figure 4.1**b-d), TMR-streptavidin binds to the microtubule surface at densities of one hundred to tens of molecules per micron of microtubule, respectively. Thus, the affinities between the biotinylated tubulin and streptavidin are similar in all four buffer and human sample assays

because $K_A = \frac{[Bt][STV]}{[Bt-STV]} - [Bt]$ where K_A is the affinity, [Bt] is the concentration of biotin in solution, [STV] is the concentration of TMR-streptavidin in solution, and [Bt-STV] is the measured amount of TMR-streptavidin bound to the microtubule surface in solution. Since the binding densities are similar in all four samples while the rest of the assay conditions remain constant, I conclude that these body fluids allow cargos to bind to the microtubule surface.

While streptavidin and avidin are not present in human body fluids, biotin is inherently found in some body fluids. Free biotin will affect the binding capacity measurement by saturating the biotin-binding sites on streptavidin, which prevents the biotin-saturated streptavidin from binding to biotinylated microtubules. Urine and blood plasma inherently contain high concentrations of biotin (on the order of 100 pM and 1 pM, respectively) highlighted in **Figure 4.1**c and d.[115, 133] Since each streptavidin binds four biotin molecules and the affinity between biotin and streptavidin is high, the depletion of biotin binding sites on streptavidin becomes relevant to the assay when the concentration of streptavidin approaches one fourth the concentration of biotin. As expected, the binding of free biotin saturates the rhodamine signal in urine and blood plasma, resulting in fewer fluorescent streptavidin bound to the microtubule surface at low (<100 pM) streptavidin concentrations.

These results show that 100 nM and 1 nM concentrations of streptavidin bind to biotinylated microtubules similarly in plain buffer, undiluted human saliva, urine, and blood plasma. Since the body fluids tested here neither sterically nor electrostatically prevent the medium sized streptavidin protein

from binding directly to the microtubule surface, I conclude that microtubule surfaces are capable of binding cargos in these medically relevant samples that are often used in point of care diagnostic tests. These observations corroborate the compatibility of antibody-functionalized microtubules as cargo-carrying microshuttles in human urine, saliva and blood plasma. Next, I looked into the motility properties of microtubules in these medically relevant biological samples.

4.3 Microtubules and Their Motility Properties in Blood Plasma, Urine, and Saliva

To investigate the transport capabilities of the kinesin-microtubule system in medically relevant samples, I performed gliding assays in a series of dilutions of blood plasma, urine, and saliva and measured their velocities. The assay chambers were prepared as previously described with a casein coat blocking the surface and NKHK560cys kinesin motors adsorb to the glass surface. Fluorescently labeled microtubules were introduced into the chamber with an ATP-containing motility solution (See **Experimental Section**) and the body fluid. At 87% body fluid the entirety of BRB80 buffer typically used in gliding assays was replaced with the body fluid. The remaining 13% of the solution consisted of microtubules and motility solution (2 mM $MgCl_2$, 0.05 mg ml^{-1} casein, 0.08 mg ml^{-1} catalase, 0.1 mg ml^{-1} glucose oxidase, 10 mM glucose, 10 mM DTT, 1 mM ATP, 20 μM paclitaxel). The microfluidic chambers were then sealed and visualized after 10 minutes. The gliding assay results are presented in **Figure 4.2** where

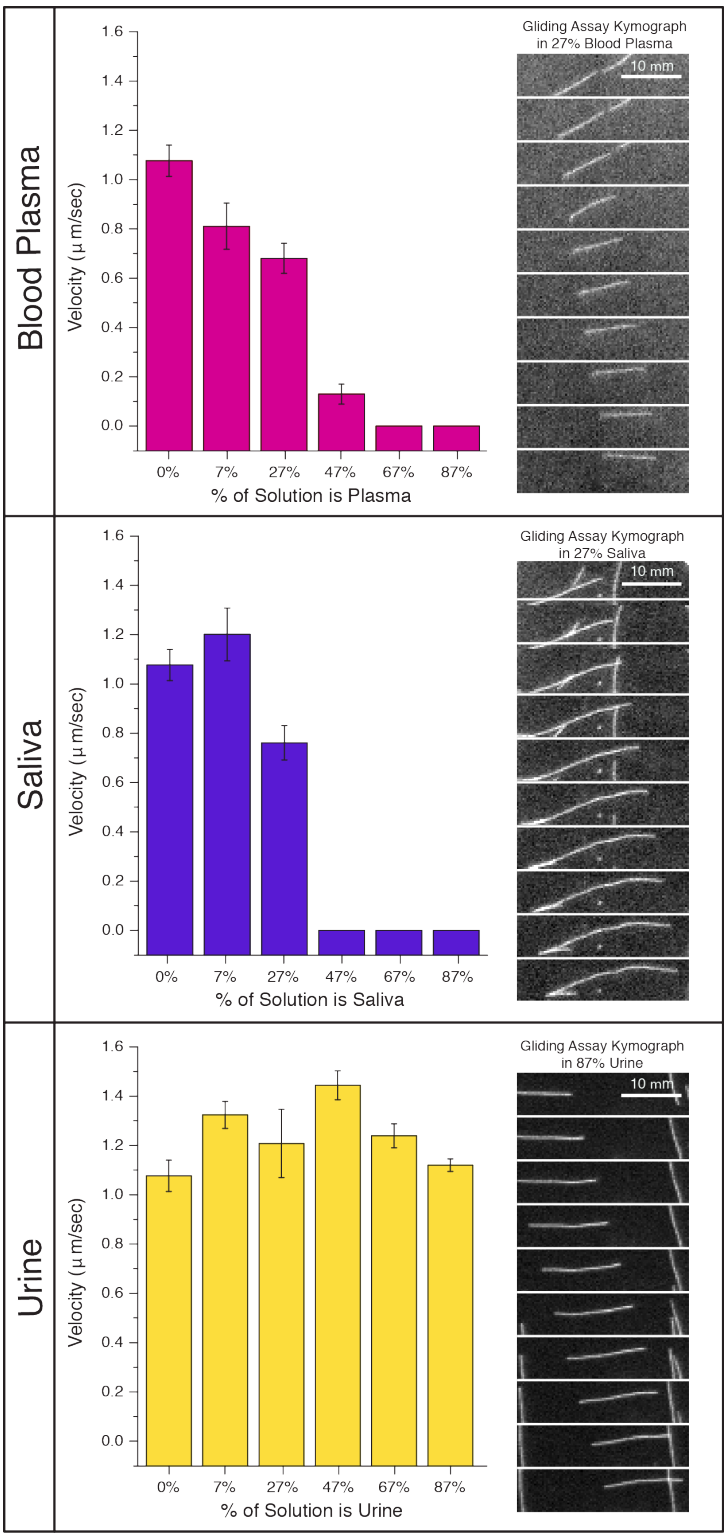

Figure 4.3 Gliding assay velocities in body fluids. Gliding assay results show that gliding assay motility deteriorates at concentrations >27% in human blood plasma (*top*) and saliva (*middle*). Gliding assay motility remains robust in urine (*bottom*).

velocities and kymographs of motile microtubules are presented for each body fluid tested. Gliding assay motility was the most robust in human urine while gliding assay velocities decrease in higher concentrations of blood plasma and saliva. Both plasma and saliva assays show that gliding assay motility stops at 67% and 47% buffer replacement, respectively, and microtubules no longer bind to the kinesin-coated surface. For these assays, the velocity is marked as 0 μm sec^{-1} with no error bars because there were no motile events to measure. When blood plasma and saliva make up 27% of the motility assay buffer, gliding assay velocities decrease significantly by 30-40%. For gliding assays performed in urine, there is no marked decline in gliding assay velocity as the urine becomes more concentrated in solution.

As discussed in Chapter 3, gliding assay velocities several hundred nanometers per second remain in the ideal range for existing kinesin-driven technologies. From these results I conclude that blood plasma, saliva, and urine all support gliding assay motility after moderate (< 10-fold) dilutions 10 minutes into the gliding assay. These results coupled with the streptavidin-binding results presented in Section 4.2 strongly suggest that human saliva, urine, and blood plasma can be diluted in assay buffer and directly used without any additional processing steps to collect and transport cargos in gliding assays.

4.4 Motility Characteristics Required for Steering Microtubules in Kinesin-Driven Technologies

Now, I will assess the potential of incorporating body fluids in existing kinesin-driven technologies. Reflecting on the existing kinesin-driven platforms

that have been developed (See Chapter 2), we recall that current designs rely on gliding assay geometries where microtubules are autonomously guided through microfluidic devices. The most developed kinesin-driven platform(s), such as those developed by Lin *et al*, depend on mechanical microtubule-barrier interactions to direct the leading end of microtubules.[72, 79, 80] Another proof-of-concept models developed by van den Heuvel *et al* steer the leading end of microtubules using electrostatic forces.[89] Both of these steering mechanisms rely on guiding the freely diffusing, leading end of the microtubule along a kinesin-coated surface (See **Figure 2.3**).[72] To be successful, the devices also require that microtubules move and be directed independently of each other and that the assay functions for approximately 1 hour.

To characterize the quality of gliding assay motility, I monitored behaviors that were present in body fluid-containing gliding assays and would prevent the microtubule tip from being effectively guided in kinesin-driven technologies. These behaviors are illustrated in **Figure 4.3** and **4.4**. I define high quality motility as microtubules gliding with constant velocities where the leading end of the microtubule is within 600 nm, or within the depth of focus of the optical set up (Zeiss Plan-Neofluar 40x/1.3 oil immersion objective excited with 590nm light), of the kinesin-coated glass surface as illustrated in the top panel of **Figure 4.3**. High quality motility is the most ideal for the microtubule tip to be effectively guided in kinesin-driven platforms because steering events have a higher probability of success and is the standard upon which existing microtubule-guiding models are based.[72]

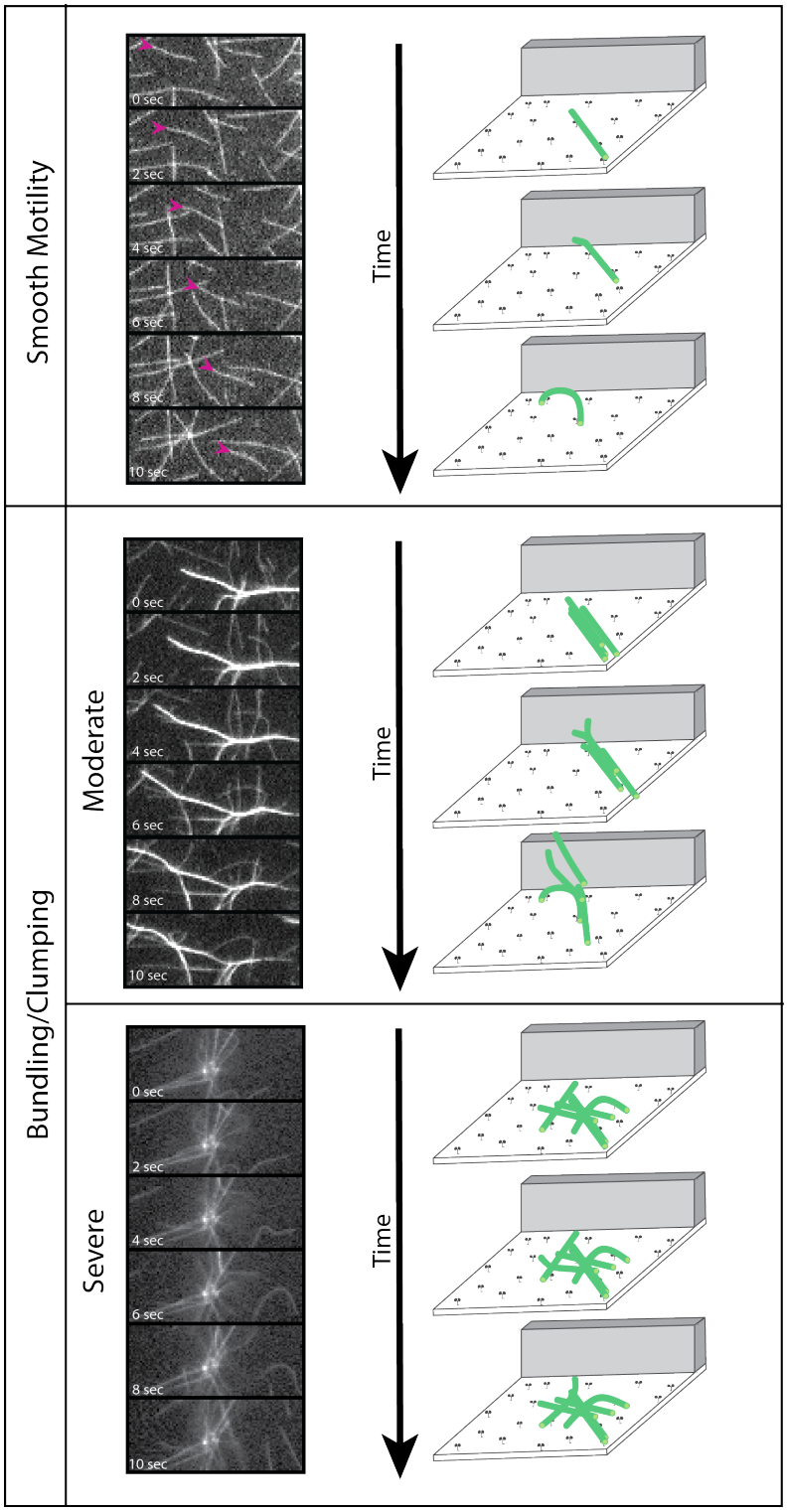

Figure 4.4 High quality motility and the effects of aggregation. *Top* High quality, smooth motility is conducive for leading MT tips to be effectively guided mechanically in gliding assays. *Bottom* Moderate MT bundling prevents MTs from being independently guided in kinesin-driven technologies. Severe aggregation halts MT motility in gliding assays.

Microtubules aggregating was an artifact observed in certain assays containing body fluids. While bundled microtubules can still remain motile as seen in the kymograph labeled "Moderate" in the bottom pane of **Figure 4.3** and in existing literature, individual microtubules cannot be distinguished and independently guided in assays where individual MT control is necessary for successful steering events.[134] Bundling can become more burdensome in assays by causing microtubule aggregates that are not parallel to each other as seen in the kymograph labeled "Severe" in the bottom pane of **Figure 4.3**. Severe bundling prevents MTs from moving in a gliding assay, and over time, these severe bundles dissociate from the kinesin-coated surface and diffuse away. Halting motility in a gliding assay and having microtubules dissociate from the kinesin-coated surface due to severe clumping is detrimental to the kinesin-driven technologies that characterize success as moving microtubules throughout a microfluidic platform. Others have explained microtubule aggregation as an artifact of either specific or nonspecific protein-protein interactions.[135-137] Specific protein-protein interactions that cause MT bundling usually involve microtubule-associated proteins (MAPs) or microtubule-based biomolecular motors. When bundling occurs in solutions that do not contain MAPs or MT-based motors, such as the body fluids used in these assays, we assume that nonspecific protein-protein interactions cause the aggregation.

Figure 4.4 illustrates a third artifact of gliding assays in body fluids called floating ends. Floating ends are not typically seen in motility assays performed in popular buffer conditions and have not been previously studied. Since floating ends are not prevalent in standard gliding assays, I assume that the floating ends

are an artifact of the protein-rich samples and not a result of imperfections in the microtubule that may cause curvature at the ends. A floating end occurs when one end of a microtubule dissociates from the kinesin-coated surface and diffuses hundreds of nanometers to microns into solution. “Moderate” floating ends diffuse into solution, eventually reattach, and continue to glide upon to the kinesin-coated surface. The yellow arrow in the kymograph marks the point where the microtubule detaches from the kinesin-coated surface and the floating end begins to the right of this point. Floating ends are considered “Severe” when the microtubule completely dissociates from the kinesin-coated surface and diffuses into solution which is not ideal for microtubule shuttles transporting cargos in kinesin-driven devices.

While MTs exhibiting moderate floating ends continue to be motile, the floating end reduces the probability of a successful steering event because of the mechanics of the system. Microtubules are naturally stiff with a persistence length of 8 millimeters.[138] Since microtubules typically used in gliding assays are tens of microns long, we can assume that a microtubule acts as an elastic cylindrical rod.[138] When bound to a kinesin-coated surface, it is energetically favorable for the stiff microtubule to remain bound to the flat, glass surface (*xy* plane). The leading tips of microtubules in gliding assays undergo thermal diffusion (**Figure 2.3**) such that the tip diffuses in solution at some angle θ in the *z*-direction. In smooth, high quality motility θ remains very small, and the freely diffusing end of the microtubule quickly binds to a kinesin motor molecule in the directed path to be successfully guided. In high quality motility, the elastic

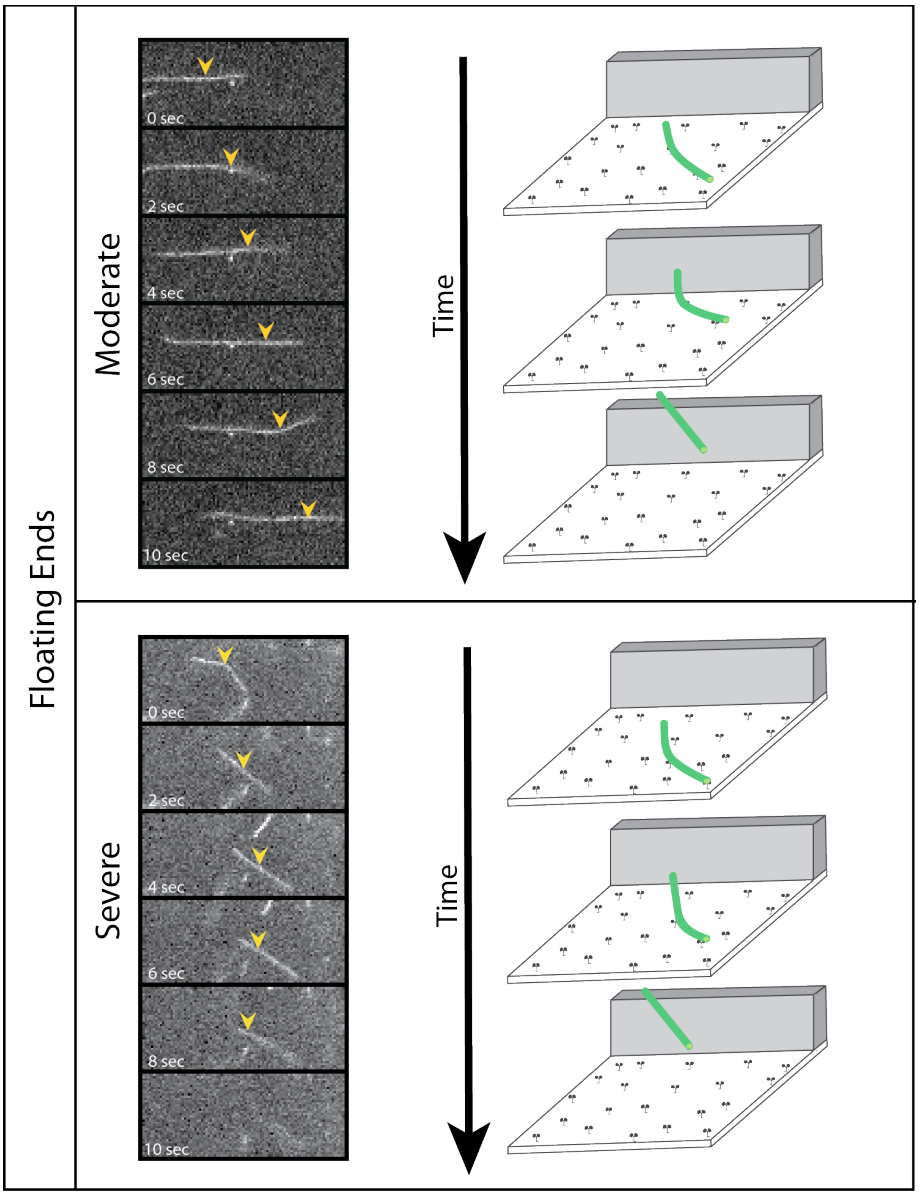

Figure 4.4 Floating ends are detrimental to guiding microtubules The yellow arrow marks where the floating end begins. In both kymographs the floating end is to the right of the arrow and diffuses freely in solution while the remainder of the MT stays bound to the kinesin-coated surface. In moderate cases, the MT can sustain gliding assay motility. Severe floating ends cause the MT to dissociate from the kinesin-coated surface.

energy due to bending is $U(\theta) >> k_B T$ where k_B is the Boltzmann constant and T is the temperature.

As a result, the restoring force overpowers thermal fluctuations and drives the stiff microtubule down to the kinesin-coated xy-plane ($\theta = 0$), assuming that kinesin is sufficiently dense and is not a limiting factor. When θ becomes larger and approaches some critical angle $\beta(\theta)$, the restoring force that drives the MT down to the more energetically favorable position ($\theta = 0$) for successful steering events can be overpowered by a drag force on the MT tip. By definition, θ for MTs with floating ends is significantly larger than θ in high quality motility. Thus, floating ends increase the probability for microtubule tips to reach microstates where $\theta \geq \beta(\theta)$, which increases the probability of having unsuccessful steering events and is undesirable for kinesin-driven technologies.

Two theories of the causation of floating ends are addressed here. First, floating ends can be an artifact of a sparsely coated kinesin surface. Defining t_k as the time it takes the MT tip to bind to the next kinesin molecule, if $t_k > {}^{l}/_{v}$ where l is the length of the portion of the microtubule bound to the kinesin-coated surface and v is the gliding velocity of the microtubule, then a floating end would be considered "severe" and the MT would dissociate from kinesin-coated surface. According to previous literature, I assume that kinesins are spaced approximately 200 nm apart from one another in the assays used in this work. This kinesin-density has been shown to promote smooth, high quality motility under typical assay conditions.[72] An alternative theory for the cause of floating ends is that proteins block the microtubule surface such that kinesin cannot

successfully bind to the microtubule surface. This would result in severe floating ends if protein blocking made t_k such that $t_k > {}^{l}/_{v}$. Functionally, the two effects are the same.

To better understand the potential of the kinesin-microtubule system in advanced immunoassay platforms, I performed an in depth analysis to characterize gliding assay motility using the three qualitative standards of motility established in this section in blood plasma, specifically. By understanding the effects blood plasma has on gliding assay motility, we can prepare samples accordingly and engineer devices to develop robust, efficient kinesin-driven devices that function in medically relevant samples.

4.5 Motility Properties of Kinesin and Microtubules in Human Blood Plasma

To assess the compatibility of blood plasma for kinesin-driven technologies, I measured the gliding speeds and the amount of bundling and floating end events that occurred in gliding assays. By tracking the number of MTs that remain motile and can be guided independently (i.e., no clumping or bundling) and efficiently via the leading end being conjugated to the kinesin-coated surface (i.e., no floating ends) over 1 hour, I can determine under which conditions blood plasma can be successfully incorporated into kinesin-driven technologies that autonomously steer microtubules. These gliding assays were performed using NKHK560cys motors, fluorescently tagged microtubules, and the same assay conditions as previously mentioned (See **Experimental Section**).

Since assays were monitored for one hour, an ATP regeneration system was incorporated into the motility buffer to ensure that changes in velocity were an effect of the blood plasma in solution and not due to depletion of ATP.

Unfiltered Blood Plasma

Gliding assay motility results are illustrated in **Figure 4.5** where blood plasma made up 5%, 1%, and 0.1% of the motility buffer. The gliding assay velocities were unaffected by the presence of blood plasma during the one hour assay (grey bars). The velocities remain constant throughout the assay, staying within one standard deviation of the initial velocity. The phosphokinase ATP regeneration system used is sufficient for maintaining robust gliding assay motility in solutions containing 5% blood plasma. Since no change in velocity is seen as the concentration of blood plasma increases by 50-fold in this assay, it appears that the kinesin motor molecules themselves are unaffected by the presence of blood plasma in the sample. Significant inhibitiors or steric or electrostatic interferences between kinesin and proteins in the blood plasma would have the following effects: increase in the presence of floating ends, slower gliding assay velocities, or terminate the gliding velocity. Since microtubule behavior is observed in this assay, directly drawing conclusions regarding the kinesin in the system would not be compelling or sound. To assess the effect blood plasma has on kinesin motor molecules, one could make single molecule observations to determine how the binding rate, velocity, and run length of kinesins are effected in blood plasma when compared to plain assay

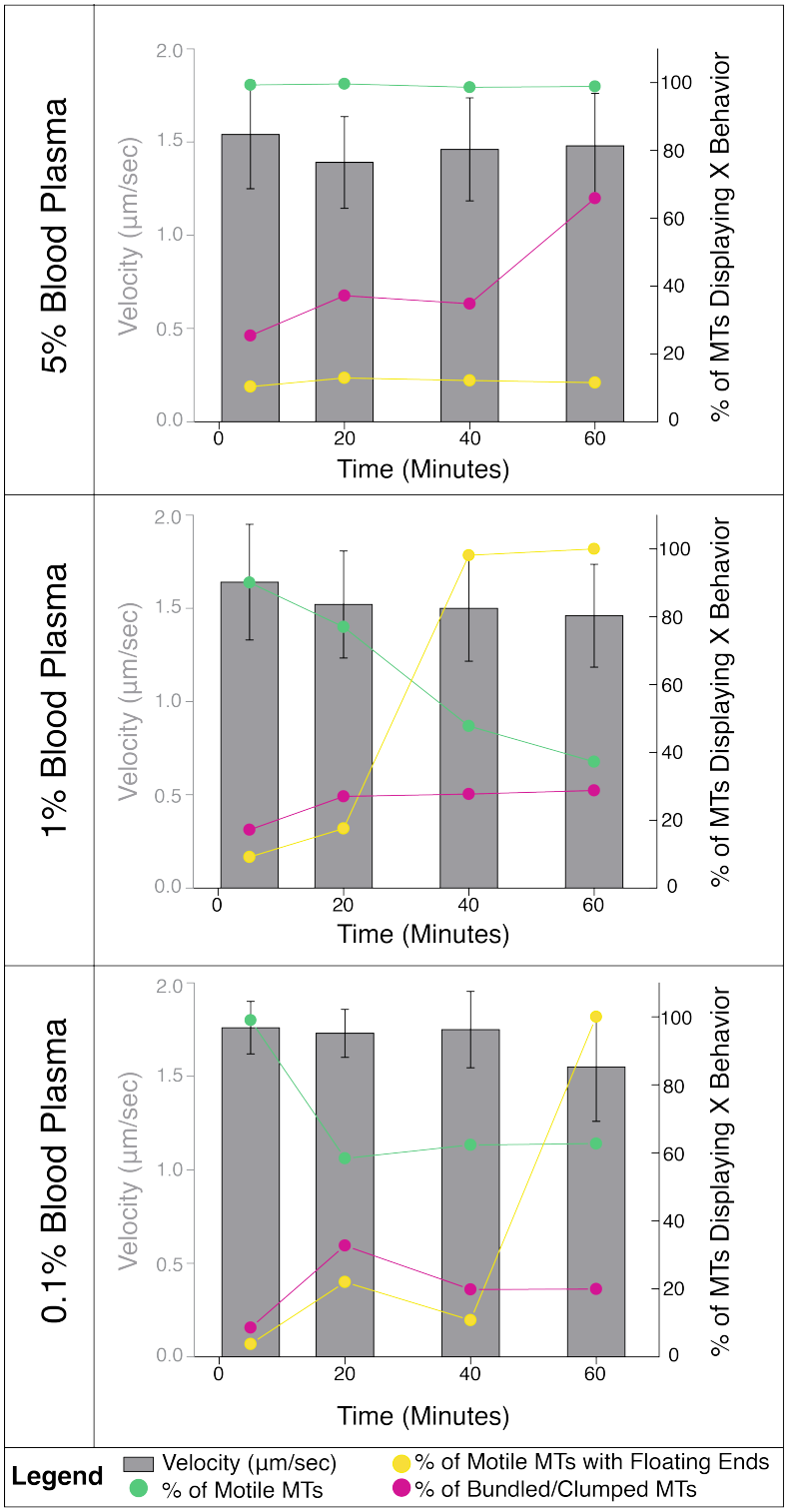

Figure 4.5 Gliding assay motility in blood plasma Gliding assay velocity (grey bars) remain constant in the presence of blood plasma. MT clumping (pink) affects the 5% plasma assay while floating ends significantly affect 1% and 0.1% assays after 60 minute long assays.

buffer. Due to the complexity of the blood plasma, it would be difficult to distinguish whether the quality of motility is affected by plasma proteins interfering with the microtubule surface or the kinesin motors themselves. Although diagnosing the exact mechanism affecting the system is limited in both gliding and single molecule assays, interpreting gliding assay results is the most appropriate method to assess the kinesin and microtubule's compatibility in blood plasma for kinesin-driven technologies that rely on gliding assay protein geometries.

Next, I look at how blood plasma affects the quality of microtubule gliding by observing detrimental behaviors outlined in Section 4.4. Shown in **Figure 4.5** MT bundling (pink circles) is significant in the more concentrated 5% assays with 66% of the MTs being clumped or bundled after an hour. As MT aggregation becomes an issue in the 5% blood plasma assay, the ratio of motile MTs in the assay remains high. Over time, severely bundled MTs dissociate from the kinesin-coated surface and diffuse away. As bundling progresses in the 5% assay, only those that are still motile are present in these observations (green circles). In the 1.0% and 0.1% assays floating ends lower the quality of motility more so than aggregation. As 100% of the microtubules in the assays have floating ends within 40 to 60 minutes in the 1% and 0.1% blood plasma assays, respectively, the motility ratios (green circles) in the gliding assay decline. The 1% and 0.1% assays have more MTs tethered to the glass surface that are not motile.

These results corroborate that blood plasma interferes with the mechanisms utilized in existing kinesin-driven technology platforms that rely on

steering microtubule tips. Because bundling dominates in the higher (5%) blood plasma concentrations, this data suggests that nonspecific protein-protein interactions affect the quality of gliding assay motility. The fact that the velocities in 1% and 0.1% blood plasma assays do not decrease suggests that the floating ends in these assays are an artifact of more moderate protein-protein interactions (instead of direct kinesin interference) which would be a direct result of further diluting the blood plasma from 5% where protein-protein interactions cause bundling. Preliminary experiments integrating 1% blood plasma into Lin's microtubule concentrator device, and these conclusions were confirmed. Microtubules on the kinesin-coated surface were motile, however the density of the microtubules in the devices significantly decreased with time. As microtubules encountered the kinesin-free barriers, they dissociated from the kinesin-coated surface instead of being steered by the barrier. The number of MTs concentrated in 1% blood plasma was <1% of those concentrated in plain assay buffer. The few that were concentrated consisted of motile microtubule bundles that successfully made their way to the concentrator regions.

Significant (1,000-fold) dilutions of plasma are not sufficient in sustaining long term (1 hour) motility assays that rely on steering microtubules because of the abundance of floating ends. Thousand-fold sample dilutions themselves are not ideal for immunoassay applications regardless of the motility effects because diluting the sample demands more sensitive detection capabilities. To exhaust the studies on the blood plasma for the proposed technologies, I looked into sample preparation techniques that result in high quality motility and are applicable for point-of-care diagnostic applications to which kinesin are so

appealing. In immunoassays a large number of biomarkers commonly used for disease detection involve a class of small molecular weight proteins called cytokines.[139] In order to keep cytokines of interest in the blood plasma sample and limiting the protein-protein interactions that likely interfered with the blood plasma gliding assay, I filtered the blood plasma using size exclusion filtration.

Filtered (10 kDa) Blood Plasma

Filtering blood plasma with a 10 kDa filter keeps 10% of the protein species and 74% of the hormone species that are inherently found in blood plasma present in the sample, which is ideal for immunoassays that detect an array of these small proteins, peptides, or steroids. The 10 kDa filtration step also keeps small molecule drugs in the blood sample which can be monitored to determine the effectiveness or status of various drug delivery systems such as chemotherapies. After filtration the blood plasma was used immediately in the same gliding assay protocol (See **Experimental Section**). The microtubule velocity and quality of motility were analyzed using the same set of qualitative standards discussed in Section 4.4. I tested 10-, 20-, and 100- fold dilutions of filtered blood plasma. Similar to the unfiltered plasma, the gliding assay velocities in filtered plasma were unaffected by the tested dilutions. The velocities for all of the tested samples were constant for one hour, all ranging within one standard deviation of the measurement. Since the unfiltered blood plasma did not alter the gliding assay velocity (See **Figure 4.5**), I expected that filtering plasma and removing proteins from the solution would either glide

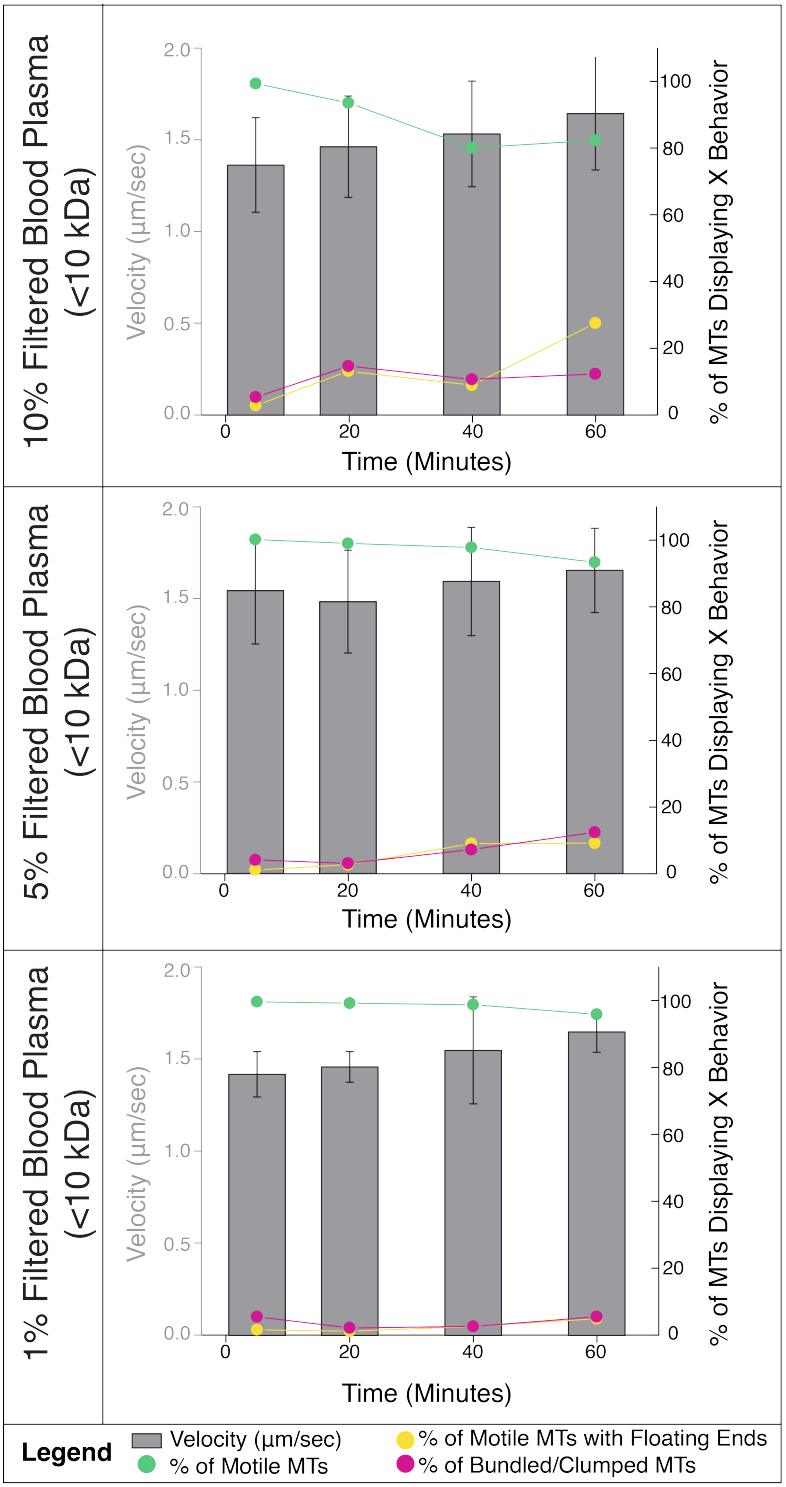

Figure 4.6 Gliding assay motility in 10 kDa filtered blood plasma. Gliding assay velocities (grey bars) are not significantly affected by incorporating filtered blood plasma in gliding assays. As time increases, floating end MTs impact the quality of motility in 10% and 5% samples while MT bundling is not an issue when compared to unfiltered blood plasma.

similarly or more robustly than in unfiltered plasma. Filtering out large proteins and ultimately reducing the total protein concentration in solution led to a significant decrease in microtubule bundling or aggregation (pink circles) where >87% of the microtubules in solution were gliding independent of each other. Additionally, the presence of floating ends (yellow circles) was significantly reduced in the filtered sample. After one hour floating ends make up 27%, 9%, and 5% of the 10-, 20-, and 100-fold diluted plasma samples, respectively. As hypothesized, reducing the concentration of plasma protein in the assay led to higher quality motility. These observations support the theory that bundling and floating ends are caused by nonspecific protein-protein interactions. As the quality of motility improves by filtering the blood plasma, the ratio of motile microtubules also increases.

4.6 Conclusions

The results presented in this Chapter indicate that microtubules can collect and transport cargos in human saliva, urine, and blood plasma for short (10 minute) time scales. I developed a method to analyze the compatibility of complex biological samples in existing kinesin-driven technologies that rely on controlling microtubule motion by steering the leading tip of the microtubule in gliding assays. After assessing the quality of motility in blood plasma and 10 kDa filtered blood plasma, I concluded that unfiltered blood plasma is not an effective sample to incorporate in such assays. To achieve high quality motility in unfiltered blood plasma, assays must be done for short periods of time (<1 hour)

and diluted 1000-fold. These large dilutions negate the benefits of performing immunoassays in blood plasma because the analyte of interest becomes diluted 1000-fold and detection limits of immunoassay platforms must compensate by becoming 100- or 1000-fold more sensitive for most assays. Robust motility that satisfies the current demands of kinesin-driven technologies is achieved through a 10- to 20-fold dilution of blood plasma that contains the proteins, peptides and steroids 10 kDa or smaller.

4.7 Experimental Section

Human Sample Preparation: Blood Plasma

Blood was drawn in a sterile environment from a trained professional per OSEH regulations in an EDTA anticoagulant coated tube (Becton Dickinson 367861). Tube was inverted several times. Blood was spun for 15 minutes at 2,000 x g at 4° C to remove blood cells and platelets. Supernatant was put in a clean tube and kept on ice until it was aliquoted and frozen at -80° C for storage. Blood plasma was thawed on ice before each assay and vortexed for several seconds before handling. When blood plasma samples were filtered, pure blood plasma was spun for 15 minutes at 5,000 x g in 10 kDa columns (Corning Spin-X) or 30 kDA columns (Amicon). The solution that was filtered out of the columns was used immediately and considered the 100% filtered plasma standard.

Human Sample Preparation: Saliva

No food or liquid was consumed 1 hour prior to collecting the saliva sample. After collection, saliva was spun at 10,000 x g for 20 minutes at 4° C. The supernatant was collected, aliquoted, and stored at -80° C. Saliva was thawed on ice before each assay and vortexed for several seconds before handling.

Human Sample Preparation: Urine

Urine was collected and centrifuged at 10,000 x g for 20 minutes at 4° C and then filtered through a 0.22 μm vacuum filter. The sample was then aliquoted and stored at -80° C until used in the assay. Urine was thawed on ice before each assay and vortexed for several seconds before handling.

Microtubule Preparation

Tubulin was purified and microtubules were polymerized as described in Chapter 3.[126] In the binding assays, tubulin was labeled with amine-reactive biotin-XX succinamadyl ester (Thermo B-1606) using the same labeling procedure used for TMR dye described in Chapter 3. Excess biotin was quenched with K-glutamate, and microtubules were removed from the label through polymerization and cycling.

Binding Capacity Assays

Microtubules polymerized with 1.87 mg ml^{-1} biotinylated tubulin and 0.13 mg ml^{-1} tetramethylrhodamine labeled tubulin. After polymerization, microtubules were spun in Beckman Airfuge at 30 psi for 30 seconds and resuspended in BRB80+T. Tetramethylrhodamine streptavidin (Invitrogen S-870) was carefully diluted for this assay as to ensure that a significant amount of protein was not lost to nonspecific binding of the streptavidin to the surface of the eppendorf tubes or pipette tips. Dilutions were done in a solution of 1.0 mg ml^{-1} biotin-free casein that will be referred to as blocking buffer. For human sample assays, dilutions were done using the same protocol except that the protein-rich human sample was used as the blocking buffer. The desired amount of blocking buffer was added to the base of the tubes in which the dilution took place and allowed to sit for several minutes to ensure that the surface of the tube was blocked. Pipette tips were coated with the blocking buffer before pipetting any solution containing streptavidin. Once streptavidin was added to the dilutions, the solution was mixed using a blocked pipette tip in the base of the tube coated with blocking buffer.

All assays were performed in a microfluidic chamber described in Chapter 3. First, a precoat of 0.1 mg ml^{-1} casein in BRB80 is flown through and sits for 3 minutes. Kinesin wash containing 0.05 mg ml^{-1} casein and excess NKHK560cys in BRB80 +T is flown through and sits for 5 minutes. Biotinylated microtubules were flown through and sit for 5 minutes followed by a BRB80 +T rinse of 5 chamber volumes to rinse away any remaining free biotin. Two chamber volumes of TMR-streptavidin diluted in blocking buffer or the human sample

being tested was flown into the chamber and incubated with the microtubules for 10 minutes. The free, unbound fluorescent streptavidin was rinsed from the chamber using 15 chamber volumes of BRB80+T. Samples were visualized using the aforementioned epifluorescence, mercury arc lamp optical set up. Image processing and measurements were done using the same protocol discussed in Chapter 3.

Motility Assays

Microfluidic flow chamber was assembled as described above. The assay begins with the same precoat and kinesin wash described above for the binding capacity protocol. Motility buffer (2 mM $MgCl_2$, 0.05 mg ml^{-1} casein, 0.08 mg ml^{-1} catalase, 0.1 mg ml^{-1} glucose oxidase, 10 mM glucose, 10 mM DTT, 1 mM ATP, 20 μM paclitaxel) containing TMR-labeled microtubules and an ATP regeneration system (0.05 mg ml^{-1} creatine phosphokinase and 10 mM phosphocreatine) was added to the specific human samples and then flown through the chamber. Dilutions of the human samples were made in BRB80 such that only the human sample itself is diluted from the solution and enzymes and chemicals (with the exception of BRB80) within the motility buffer remain at constant concentrations. The chamber is sealed with hot wax and sits for 5 minutes before visualizing. Image sequences were taken on the aforementioned optical set up.

Quality of Motility

Motility assays were run as described above. Data was collected in 10 frames with 2 seconds between each frame at the mentioned time intervals. The videos were analyzed by eye where each event was counted during the 20 sec clip. Tethered or floating events included any event that did not move or had a floating end for at least 6 seconds. The total number of microtubules observed were those counted in the first frame and used as the total number of MTs throughout the entire analysis for that 20 sec video.

CHAPTER 5
CONCLUSIONS AND FUTURE WORK

The work presented in this dissertation makes a clear step forward in the direction of implementing a kinesin-driven active transport system into a realistic immunoassay platform to detect ultralow analyte concentrations. This progress is promising for the implementation of such a device in resource-limited settings where assays must be done quickly with noninvasive samples and without electricity at ambient temperatures. Before a kinein-microtubule based immunoassay platform can be implemented in clinical settings there are two key barriers that must be overcome. Here, I will discuss the necessary future steps to detect analyte that is not directly labeled (Section 5.2) and in better incorporating the microtubule-kinesin system into medically relevant samples (Section 5.3). The section will conclude with suggestions for future directions kinesin-driven systems should progress.

5.1 Conclusions

The work presented in this thesis critically contributes to the field of biomolecular motor-driven technologies. While scientists and engineers have

developed the kinesin-microtubule system to serve as an active transport system for LOC technologies, there existed voids in previous work that prevented the system from being implemented into clinical settings, specifically a more thorough, quantitative analysis assessing the detection potential of antibody functionalized microtubules and the compatibility of the protein systems in medically relevant samples. In this work a protocol was developed to covalently link antibodies to microtubules that was designed to prevent undesired crosslinking events which results in simple handling procedures, faster assay times, and cheaper assays. Furthermore, the antigen binding capabilities of the functionalized microtubules were thoroughly quantitatively analyzed to conclude that microtubules could, in fact, be used to capture ultralow (fM) concentrations of antigen. The second portion of this work looked at the ability for microtubules to bind cargos and be transported in gliding assays in human blood plasma, urine, and saliva. The results show that microtubules can, in fact, capture and transport cargos in these medically relevant samples. A set of criterion was established to characterize the effect body fluids have on gliding assays that is reflective of the demands for current kinesin-driven technologies. The method of analysis should serve as a standard for future kinesin-microtubule-body fluid compatibility studies as it gives a unique insight to the potential the body fluid has on being integrated into kinesin-driven technologies.

The quantitative analyses performed throughout this dissertation work are novel and were necessary in establishing the kinesin-microtubule system as a platform for immunoassays. Here, I will address the future work that needs to be done in developing an ELISA-based device that takes advantage of the kinesin-microtubule system that is ready for clinical use. I begin by exploring the work

needed to broadly detect and transport antigen labeled with a detection antibody. Then, the necessary engineering that needs to be done to create a micro- or nanofluidic device that harnesses the body fluid motility results presented will be discussed.

5.2 Future Work: Fluorescent Detection Via Labeled Detection Antibodies

As addressed in Chapter 3 a thorough study exploring gliding assay motility with antibody-sandwich constructs tethered to the microtubule surface should be explored to most effectively implement the antibody functionalized MTs into clinical settings. The assays in this dissertation demonstrated robust motility when antibodies tethered to MTs were carrying fluorescently tagged antigens. In clinical settings, labeling the antigen directly is unrealistic. If one were to specifically label the antigen, which would require purifying the protein from the sample, the immunoassay itself would become unnecessary since the protein would be extracted through other means. Using a fluorescently tagged detection antibody to specifically label the antigen is the current standard for immunoassays and is ideal. In this study I discovered that the large antibody sandwich constructs present in high densities sterically hinder the microtubule-kinesin interaction in the given assay conditions, which prevents gliding assay motility. Other researchers have been able to successfully transport large cargos such as beads, vesicles, and cells, but the labeling density of their microtubules is significantly less and the kinesins maneuver around individual cargos.[18, 25, 60] To sustain motility, the binding density of the analyte could be reduced so that kinesin can accommodate for and move around the large cargo in order to

transport these larger constructs. Since reducing the antibody density sacrifices the detection limit of the system (Chapter 3.3), I will now explore ways in which motility can be sustained while maintaining a high concentration of antibody in solution.

Modifying Assay Geometry to Support the Transport of Large Cargos

The gliding assays reported here were all performed using a 560 amino acid long truncated kinesin-1 motor protein. As a result, the motor domains of the truncated motor rest very close (~7 nm) to the glass surface that is imaged in a gliding assay.[140] A full-length kinesin-1 motor protein is over 900 amino acids long and has a length of 58 nm. Using the truncated motor, the long coiled-coiled tail domain that makes up 86% of the length of the kinesin motor is not present. Since my results (Chapter 4) suggest that sandwich assay motility issues arise from steric hindrances, I believe that using a longer or full length kinesin motor will promote the transport of larger cargos bound to the microtubule surface will by distancing the functionalized microtubule further from the glass surface. Because the truncated kinesin are able to support robust motility on a microtubule with 5-10% of dimers functionalized, my results suggest that longer kinesin constructs could accommodate for a similar density of larger protein complexes assuming that longer kinesin molecules are bound to the glass surface at a similar density.

Modifying MT-Antibody Conjugation Procedure to Support the Transport of Large Cargos

Modifying the microtubule-labeling procedure to change the geometry of the labeling system may be sufficient in supporting antibody-sandwich assay motility without significantly sacrificing the detection capabilities of the system. Single molecule studies show that kinesin step linearly along the microtubule protofilament.[141] We can take advantage of the gliding assay geometry by attaching large cargos to half of the microtubule and leaving the other half of the microtubule along the cylindrical axis free for kinesin to bind and step along. The existing protocol (Chapter 3.2) functionalizes microtubules as they diffuse freely in solution such that the MT labeling is uniform along the MT surface. An alternative to this method would be to functionalize MTs while they are bound to a kinesin coated surface using an ATP analog, such as adenosine 5′-(β,ϒ-imido)triphosphate (AMP-PNP), would hold the MT to the surface throughout the entire procedure. Using the same assay geometry as the binding capacity assays (**Figure 3.2**), 10 μM AMP-PNP can be added to solution to securely bind the microtubules to the kinesin-coated surface. Then, the entire conjugation procedure can be done in a glass assay chamber such that the surface of the MT that is bound to the kinesin remains unfunctionalized.

To avoid SMCC crosslinker from binding to kinesin motor, the SMCC-labeling portion of the protocol can be performed outside of the assay chamber. SMCC-coated microtubules can then be added to the assay chamber for antibody functionalization. SMCC densely bound to the entire surface of the microtubule does not threaten to motility since the crosslinker does not significantly affect motility (**Figure 3.5**). Alternatively, if one wants to perform the entire labeling

procedure in an assay chamber, engineered kinesin that limit the number of exposed amine binding sites or are cysteine-free can be used to limit crosslinker from binding to kinesin. Cysteine-free motors have been engineered and are proven to sustain motility in gliding assays.[142]

Because the kinesin are bound to one side of the microtubule, antibodies will not be able to bind along the same protofilament to which the kinesin molecules are bound, leaving a lateral surface along the microtubule free from antibodies. Assuming that the kinesin coated surface binds to the two nearest protofilaments that lie closest to the NKHK560cys kinesin-coated surface and that reduced antibodies occupy a volume of approximately 14 nm x 5 nm x 4 nm, the reduced sulfhydryl groups on the antibody will be unable to reach the three protofilaments lying closest to the kinesin coated surface of the microtubule.[143] When three of the thirteen tubulin protofilaments are blocked from binding antigen, the binding capacity of the microtubule would be theoretically reduced by 23%. Recall that we define R as the concentration of antibody (receptor) in solution, L as the concentration of antigen (ligand) in solution, and C, the concentration of bound antibody-antigen. The kinetics of our system are

$$\frac{dC}{dt} = k_{on}RL - k_{off}C.$$

At equilibrium ($\frac{dC}{dt} = 0$), neglecting the effect of ligand depletion and assuming this limit is asymptotically approached for $t \gg (k_{on}L_{total} + k_{off})^{-1}$, then

$$C_{equilibrium} = \frac{R_{total}L_{total}}{K_D + L_{total}}.$$

Therefore, reducing the total concentration of antibodies, R_{total}, in solution directly reduces the number of bound antigen, C, which ultimately correlates to

the detection limit of the assay. Using realistic antibody densities established in this work coupled with a 23% reduction in binding capacity due to the modified protocol discussed above, a 10 nL sample containing 5 mm of functionalized MTs holding 86 antibodies μm^{-1} (23% of the maximum 122 antibodies μm^{-1} established previously) would capture five of the six antigen molecules found in a 1 fM antigen solution after a 25 minute incubation. This calculation also assumes that the antibody-antigen complex has a dissociation constant (K_D) ≤ 100 pM and the only antibodies in the system are those on the MT surface. Therefore, functionalizing microtubules with antibodies while the microtubules are bound to a kinesin coated surface would still create functionalized microtubules capable of capturing ultralow concentrations of antigen while supporting the transport of large cargos.

Performing the conjugation procedure in an assay chamber will require that assay conditions be re-optimized. Incubation times will need to be adjusted to accommodate for the fact that microtubule diffusion is no longer occurring. While the SMCC and antibody excesses optimized in this assay will serve as a good standard, the conditions should be optimized again to maximize the binding capacity of the system. Lastly, since pelleting the microtubules is no longer an option given this conjugation protocol, rinse steps should be optimized to sufficiently rid the system of excess antibodies and crosslinkers that may interfere with the specificity and detection capabilities of the system. If the functionalized microtubules are going to be used in the same assay chamber that they were functionalized, it is also necessary to ensure that the conjugation procedure does not prevent kinesin motility. Leaving kinesin at room

temperature for long periods of time (several hours) will negatively impact kinesin motility. But once optimized, this modified procedure could produce antibody-functionalized microtubules that sustain motility with large, sandwich assay constructs as cargos.

Transport Fewer, Larger Cargos to Sustain Motility

Instead of coating the entire surface of the microtubule with antibody sandwich constructs, one alternative is to change the geometry of the system such that antibody functionalized microspheres are transported by the microtubules. Microspheres can be functionalized with the antibody of interest along with a small portion of anti-tubulin antibodies that can bind to the microtubule.[12] Binding fewer antibody-functionalized microspheres on the microtubule would allow for the microtubule to carry fewer large cargos and maintain a high binding antigen binding capacity and, theoretically, not sacrifice motility. The size and binding density of the bead can be optimized to realize similar (fM) detection limits as the antibody functionalized microtubules.

5.3 Future Work: Kinesin-Driven Immunoassay Platforms in Blood Plasma

As discussed in Chapter 4, existing kinesin-driven platforms that autonomously guide microtubules have limited potential to function in blood plasma due to the long term (60 minute) effects blood plasma has on the quality of gliding assays. Urine looks like a promising body fluid to further characterize and determine if urine-based diagnostic tests are a more appropriate platform for

kinesin-driven immunoassay technologies. Other samples that have not been explored by researchers include cerebrospinal fluid and various types of cell lysates. However, because blood derivatives are the existing standard and currently offer the broadest application for immunoassays, determining how to best incorporate kinesin and microtubules into blood derivatives is imperative in advancing the field. As a result, we must assess the known limitations of kinesin-driven technologies in blood plasma to determine in what direction future technologies should proceed.

Separate Sample Collection from Gliding Assays

Since gliding assay motility in blood plasma deteriorates over time, researchers could separate protein collection, or cargo loading, onto the microtubule surface from motility. One way this can be accomplished is by loading cargos directly onto the microtubule surface while the microtubules are held in place on a kinesin-coated surface. Microtubule bundling and aggregation is dependent on microtubules interacting with one another. While bound in rigor, the microtubules will not have the opportunity to collide with each other as the analyte binds to the microtubule surface. However, being bound to a surface in rigor does not prevent nonspecific protein-protein interactions from occurring, which can cause bundling and floating ends as soon as the microtubules become motile. Since the working hypothesis driving the conclusions in Chapter 4 is that nonspecific protein-protein interactions drive the deterioration of gliding assay motility, several control experiments must be

performed to determine if the microtubules and kinesin can recover from being exposed to blood plasma. Removing the kinesin-microtubule system completely from blood derivatives is another option.

Microtubules can be completely removed from blood derivatives by using a collection mechanism such as an antibody-functionalized microsphere instead of functioning the microtubule itself (discussed above) that can be exposed to the sample. Microspheres functionalized with antibodies can diffuse freely in body fluids without aggregating.[144] After binding the analyte of interest, the microspheres can be pelleted out of the sample solution and rinsed through centrifugation steps or using a magnet if the beads are paramagnetic. Once the beads carrying the analyte are removed from the blood plasma, the beads can bind to microtubules through an anti-tubulin antibody or a biotin-streptavidin linkage.

Engineer Technologies Accommodating for Motility in Blood Plasma

By understanding how gliding assay motility changes over time (Chapter 4.4), engineers can design kinesin-driven technologies to accommodate for these characteristics. For example, engineering a kinesin-driven device that runs in 1% unfiltered blood plasma for 20 minutes would lead to only a 14% decrease in microtubule density with nearly 70% of the microtubules having high quality motility, allowing them to be effectively guided via mechanical or electrostatic interactions as previously discussed. Reducing the length scales of future kinesin-driven technologies such that assays are completed in 20 minutes instead

of an hour could be sufficient in sustaining motility in medically relevant samples without requiring excessive dilutions or filtration.

Removing the importance of high quality motility for microtubule control or the need to steer microtubules altogether could accommodate blood plasma samples. Instead of the proposed mechanism where a fluorescent signal from cargo-carrying MTs would be used for protein detection, researchers could, instead, engineer a system where motility itself detects the analyte of interest. This could be done by engineering a protein-signaling cascade that releases or produces ATP to power the kinesin motors or engineering a microtubule tether that releases the microtubule in the presence of an analyte "key" are just two examples as to how motility can be used as an analyte signal. Kinesin motor molecules can be engineered to have a key mechanism that switches the motor from being inhibited to uninhibited and free to traverse along the microtubule. Previous work in developing engineered motility switches for the kinesin-microtubule system is discussed in Chapter 2.1. Taking advantage of advanced bioengineering principles can transform the gliding assay geometry into a platform for analyte detection in blood plasma with a binary signal (motility and no motility). One downfall to these systems is that they would have to be highly specific to the analyte, which would make developing a platform that can detect multiple analytes laborious and expensive.

Alternatively, the assay geometry could be reversed to accommodate for the demonstrated robust kinesin motility in blood plasma. By tethering microtubules onto a coverglass for kinesin to travel upon, MT aggregation or floating ends seen in gliding assays would no longer be relevant. Instead of

microtubules serving as microshuttles carrying the cargos, the kinesin motors could be engineered to collect and carry specific cargos just as they do naturally in biological cells. Individual kinesin motor molecules are not ideal for millimeter-scale transport because, depending on the motor, they processively move for tens of nanometers to microns. However, if many motors are conjugated to a single cargo, the length of their runs increases.[145] Since the gliding assay geometry is the assay substrate that engineers have built kinesin-driven technologies upon, a lot of engineering would need to go into controlling the motion of kinesin and the placement of microtubule tracks in a reversed assay geometry.

5.4 Future Outlook for Kinesin-Driven Technologies

As biologists, engineers, and biophysicists continue to study the complex intracellular transport system, the potential for incorporating biomolecular motors into microfluidic technologies will grow. Inside a biological cell the kinesin and microtubule system are highly regulated and support advanced, energy efficient transport functions. As we better understand how these systems are regulated and controlled, we can incorporate these mechanisms into lab on chip devices. As we wait for the secrets of the biology to unravel, engineers have the capabilities to manipulate and create advanced biological systems from scratch. So long as the field continues with innovation and persistence, the kinesin and microtubule system have significant potential for improving POC

medical devices over the next several decades as engineering and biology progress together.

WORKS CITED

1. Erickson, D. and D.Q. Li, Integrated microfluidic devices. Analytica Chimica Acta, 2004. 507(1): p. 11-26.
2. Lion, N., T.C. Rohner, L. Dayon, I.L. Arnaud, E. Damoc, N. Youhnovski, Z.Y. Wu, C. Roussel, J. Josserand, H. Jensen, J.S. Rossier, M. Przybylski, and H.H. Girault, Microfluidic systems in proteomics. Electrophoresis, 2003. 24(21): p. 3533-3562.
3. Pavlickova, P., E.M. Schneider, and H. Hug, Advances in recombinant antibody microarrays. Clinica Chimica Acta, 2004. 343(1-2): p. 17-35.
4. Sanchez-Carbayo, M., Antibody arrays: Technical considerations and clinical applications in cancer. Clinical Chemistry, 2006. 52(9): p. 1651-1659.
5. Sanders, G.H.W. and A. Manz, Chip-based microsystems for genomic and proteomic analysis. Trac-Trends in Analytical Chemistry, 2000. 19(6): p. 364-378.
6. Stoll, D., M.F. Templin, J. Bachmann, and T.O. Joos, Protein microarrays: Applications and future challenges. Current Opinion in Drug Discovery & Development, 2005. 8(2): p. 239-252.
7. Wilson, D.S. and S. Nock, Functional protein microarrays. Current Opinion in Chemical Biology, 2002. 6(1): p. 81-85.
8. Schmechel, D., R.L. Gorny, J.P. Simpson, T. Reponen, S.A. Grinshpun, and D.M. Lewis, Limitations of monoclonal antibodies for monitoring of fungal aerosols using Penicillium brevicompactum as a model fangus. Journal of Immunological Methods, 2003. 283(1-2): p. 235-245.
9. Zhou, F., M. Wang, L. Yuan, Z. Cheng, Z. Wu, and H. Chen, Sensitive sandwich ELISA based on a gold nanoparticle layer for cancer detection. Analyst, 2012. 137(8): p. 1779-1784.

10. Zhu, L. and E.V. Anslyn, Signal amplification by allosteric catalysis. Angewandte Chemie-International Edition, 2006. 45(8): p. 1190-1196.
11. Barletta, J.M., D.C. Edelman, and N.T. Constantine, Lowering the detection limits of HIV-1 viral load using real-time Immuno-PCR for HIV-1 p24 antigen. American Journal of Clinical Pathology, 2004. 122(1): p. 20-27.
12. Chan, C.P.-y., Y.-c. Cheung, R. Renneberg, and M. Seydack, *New trends in immunoassays*, in *Biosensing for the 21st Century*, R.L.F. Renneberg, Editor 2008. p. 123-154.
13. Schweitzer, B., S. Roberts, B. Grimwade, W.P. Shao, M.J. Wang, Q. Fu, Q.P. Shu, I. Laroche, Z.M. Zhou, V.T. Tchernev, J. Christiansen, M. Velleca, and S.F. Kingsmore, Multiplexed protein profiling on microarrays by rolling-circle amplification. Nature Biotechnology, 2002. 20(4): p. 359-365.
14. Bachand, G.D., H. Hess, B. Ratna, P. Satir, and V. Vogel, "Smart dust" biosensors powered by biomolecular motors. Lab on a Chip, 2009. 9(12): p. 1661-1666.
15. van den Heuvel, M.G.L. and C. Dekker, Motor proteins at work for nanotechnology. Science, 2007. 317(5836): p. 333-336.
16. Hess, H., G.D. Bachand, and V. Vogel, Powering nanodevices with biomolecular motors. Chemistry-a European Journal, 2004. 10(9): p. 2110-2116.
17. Hess, H. and V. Vogel, Molecular shuttles based on motor proteins: active transport in synthetic environments. Journal of biotechnology, 2001. 82(1): p. 67-85.
18. Vogel, V. and H. Hess, *NanoShuttles: Harnessing motor proteins to transport cargo in synthetic environments*, in *Controlled Nanoscale Motion*, H. Linke and A. Mansson, Editors. 2007. p. 367-383.
19. Agarwal, A. and H. Hess, Biomolecular motors at the intersection of nanotechnology and polymer science. Progress in Polymer Science, 2010. 35(1-2): p. 252-277.

20. Bruce Alberts, A.J., Julian Lewis, Martin Raff, Keith Roberts, and Peter Walter, *Molecular Biology of the Cell*. 5th ed2002, New York: Garland Science.
21. Ronald Vale, T.F., Daniel Pierce, Laura Romberg, Yoshie Harada & Toshio Yanagida, Direct observation of single kinesin molecules moving along microtubules. Letters to Nature, 1996. 380(4 April): p. 451-453.
22. Rosi, N.L. and C.A. Mirkin, Nanostructures in biodiagnostics. Chemical Reviews, 2005. 105(4): p. 1547-1562.
23. Fischer, T., A. Agarwal, and H. Hess, A smart dust biosensor powered by kinesin motors. Nature Nanotechnology, 2009. 4(3): p. 162-166.
24. Goel, A. and V. Vogel, Harnessing biological motors to engineer systems for nanoscale transport and assembly. Nature Nanotechnology, 2008. 3(8): p. 465-475.
25. Korten, T., A. MÂnsson, and S. Diez, Towards the application of cytoskeletal motor proteins in molecular detection and diagnostic devices. Current Opinion in Biotechnology, 2010. 21(4): p. 477-488.
26. Bohm, K.J., J. Beeg, G.M. zu Horste, R. Stracke, and E. Unger, Kinesin-driven sorting machine on large-scale microtubule arrays. Ieee Transactions on Advanced Packaging, 2005. 28(4): p. 571-576.
27. Hancock, W.O. and J. Howard, Processivity of the motor protein kinesin requires two heads. Journal of Cell Biology, 1998. 140(6): p. 1395-1405.
28. Hancock, W.O. and J. Howard, Kinesin's processivity results from mechanical and chemical coordination between the ATP hydrolysis cycles of the two motor domains. Proceedings of the National Academy of Sciences of the United States of America, 1999. 96(23): p. 13147-13152.
29. Jia, L.L., S.G. Moorjani, T.N. Jackson, and W.O. Hancock, Microscale transport and sorting by kinesin molecular motors. Biomedical Microdevices, 2004. 6(1): p. 67-74.
30. Uppalapati, M., Y.-M. Huang, T.N. Jackson, and W.O. Hancock, Enhancing the stability of kinesin motors for microscale transport applications. Lab on a Chip, 2008. 8(2): p. 358-361.

31. Uppalapati, M., Y.-M. Huang, S. Shastry, T.N. Jackson, and W.O. Hancock, *Microtubule Motors in Microfluidics*. Methods in Bioengineering: Biomicrofabrication and Biomicrofluidics, ed. J.D. Zahn2010. 311-337.
32. Malcos, J.L. and W.O. Hancock, Engineering tubulin: microtubule functionalization approaches for nanoscale device applications. Applied Microbiology and Biotechnology, 2011. 90(1): p. 1-10.
33. Bachand, G.D., S.B. Rivera, A. Carroll-Portillo, H. Hess, and M. Bachand, Active capture and transport of virus particles using a biomolecular motor-driven, nanoscale antibody sandwich assay. Small, 2006. 2(3): p. 381-385.
34. Taira, S., Y.-Z. Du, Y. Hiratsuka, K. Konishi, T. Kubo, T.Q.P. Uyeda, N. Yumoto, and M. Kodaka, Selective detection and transport of fully matched DNA by DNA-loaded microtubule and kinesin motor protein. Biotechnology and Bioengineering, 2006. 95(3): p. 533-538.
35. Diez, S., C. Reuther, C. Dinu, R. Seidel, M. Mertig, W. Pompe, and J. Howard, Stretching and transporting DNA molecules using motor proteins. Nano Letters, 2003. 3(9): p. 1251-1254.
36. Dinu, C.Z., J. Opitz, W. Pompe, J. Howard, M. Mertig, and S. Diez, Parallel manipulation of bifunctional DNA molecules on structured surfaces using kinesin-driven microtubules. Small, 2006. 2(8-9): p. 1090-1098.
37. Yokokawa, R., J. Miwa, M.C. Tarhan, H. Fujita, and M. Kasahara, DNA molecule manipulation by motor proteins for analysis at the single-molecule level. Analytical and Bioanalytical Chemistry, 2008. 391(8): p. 2735-2743.
38. Agarwal, A., P. Katira, and H. Hess, Millisecond Curing Time of a Molecular Adhesive Causes Velocity-Dependent Cargo-Loading of Molecular Shuttles. Nano Letters, 2009. 9(3): p. 1170-1175.
39. Boal, A.K., G.D. Bachand, S.B. Rivera, and B.C. Bunker, Interactions between cargo-carrying biomolecular shuttles. Nanotechnology, 2006. 17(2): p. 349-354.
40. Bachand, G.D., S.B. Rivera, A.K. Boal, J. Gaudioso, J. Liu, and B.C. Bunker, Assembly and transport of nanocrystal CdSe quantum dot

nanocomposites using microtubules and kinesin motor proteins. Nano Letters, 2004. 4(5): p. 817-821.

41. Ramachandran, S., K.H. Ernst, G.D. Bachand, V. Vogel, and H. Hess, Selective loading of kinesin-powered molecular shuttles with protein cargo and its application to biosensing. Small, 2006. 2(3): p. 330-334.
42. Soto, C.M., B.D. Martin, K.E. Sapsford, A.S. Blum, and B.R. Ratna, Toward single molecule detection of staphylococcal enterotoxin B: Mobile sandwich immunoassay on gliding microtubules. Analytical Chemistry, 2008. 80(14): p. 5433-5440.
43. Liu, H., E.D. Spoerke, M. Bachand, S.J. Koch, B.C. Bunker, and G.D. Bachand, Biomolecular Motor-Powered Self-Assembly of Dissipative Nanocomposite Rings. Advanced Materials, 2008. 20(23): p. 4476-4481.
44. Hess, H., J. Clemmens, C. Brunner, R. Doot, S. Luna, K.H. Ernst, and V. Vogel, Molecular self-assembly of "nanowires" and "nanospools" using active transport. Nano Letters, 2005. 5(4): p. 629-633.
45. Rios, L. and G.D. Bachand, Multiplex transport and detection of cytokines using kinesin-driven molecular shuttles. Lab on a Chip, 2009. 9(7): p. 1005-1010.
46. Carroll-Portillo, A., M. Bachand, and G.D. Bachand, Directed Attachment of Antibodies to Kinesin-Powered Molecular Shuttles. Biotechnology and Bioengineering, 2009. 104(6): p. 1182-1188.
47. Liepelt, S. and R. Lipowsky, Kinesin's network of chemomechanical motor cycles. Physical Review Letters, 2007. 98(25): p. 258102-258102.
48. Romberg, L. and R.D. Vale, CHEMOMECHANICAL CYCLE OF KINESIN DIFFERS FROM THAT OF MYOSIN. Nature, 1993. 361(6408): p. 168-170.
49. Adio, S., J. Reth, F. Bathe, and G. Woehlke, Review: regulation mechanisms of Kinesin-1. Journal of Muscle Research and Cell Motility, 2006. 27(2): p. 153-160.
50. Hirokawa, N., R. Nitta, and Y. Okada, The mechanisms of kinesin motor motility: lessons from the monomeric motor KIF1A. Nature Reviews Molecular Cell Biology, 2009. 10(12): p. 877-884.

51. Reilein, A.R., S.L. Rogers, M.C. Tuma, and V.I. Gelfand, *Regulation of molecular motor proteins*, in *International Review of Cytology - a Survey of Cell Biology, Vol 204*, K.W. Jeon, Editor 2001. p. 179-238.
52. Verhey, K.J. and T.A. Rapoport, Kinesin carries the signal. Trends in Biochemical Sciences, 2001. 26(9): p. 545-550.
53. Brunner, C., C. Wahnes, and V. Vogel, Cargo pick-up from engineered loading stations by kinesin driven molecular shuttles. Lab on a Chip, 2007. 7(10): p. 1263-1271.
54. Hiyama, S., T. Inoue, T. Shima, Y. Moritani, T. Suda, and K. Sutoh, Autonomous Loading, Transport, and Unloading of Specified Cargoes by Using DNA Hybridization and Biological Motor-Based Motility. Small, 2008. 4(4): p. 410-415.
55. Schmidt C and Vogel V, Molecular shuttles powered by motor proteins: loading and unloading stations for nanocargo integrated into one device. (1473-0197 (Print)).
56. Hiyama, S., R. Gojo, T. Shima, S. Takeuchi, and K. Sutoh, Biomolecular-Motor-Based Nano- or Microscale Particle Translocations on DNA Microarrays. Nano Letters, 2009. 9(6): p. 2407-2413.
57. Hiyama, S., T. Inoue, T. Shima, Y. Moritani, T. Suda, and K. Sutoh, Autonomous molecular sorting by DNA labeled microtubules. Biophysical Journal, 2007: p. 331A-331A.
58. Hiyama, S., Y. Moritani, R. Gojo, S. Takeuchi, and K. Sutoh, Biomolecular-motor-based autonomous delivery of lipid vesicles as nano- or microscale reactors on a chip. Lab on a Chip, 2010. 10(20): p. 2741-2748.
59. Hiyama, S., Y. Moritani, S. Takeuchi, and K. Sutoh, *Selective Capture and Transport of Lipid Vesicles by Using DNAs and Biomolecular Motors*. Fourth International Conference on Quantum, Nano and Micro Technologies: Icqnm 2010, Proceedings, ed. V. Ovchinnikov2010. 23-26.
60. Hiyama, S., S. Takeuchi, R. Gojo, T. Shima, K. Sutoh, and Ieee, *Biomolecular motor-based cargo transporters with loading/unloading mechanisms on a micro-patterned DNA array*, in *Mems 2008: 21st Ieee International Conference on Micro Electro Mechanical Systems, Technical Digest*2008. p. 144-147.

61. Ionov, L., M. Stamm, and S. Diez, Reversible Switching of Microtubule Motility Using Thermoresponsive Polymer Surfaces. Nano Letters, 2006. 6(9): p. 1982-1987.
62. Rahim, M.K.A., T. Kamei, and N. Tamaoki, Dynamic photo-control of kinesin on a photoisomerizable monolayer - hydrolysis rate of ATP and motility of microtubules depending on the terminal group. Organic & Biomolecular Chemistry, 2012. 10(16): p. 3321-3331.
63. Hess, H., J. Clemmens, D. Qin, J. Howard, and V. Vogel, Light-controlled molecular shuttles made from motor proteins carrying cargo on engineered surfaces. Nano Letters, 2001. 1(5): p. 235-239.
64. Korten, T., W. Birnbaum, D. Kuckling, and S. Diez, Selective Control of Gliding Microtubule Populations. Nano Letters, 2012. 12(1): p. 348-353.
65. Fan, R., O. Vermesh, A. Srivastava, B.K.H. Yen, L. Qin, H. Ahmad, G.A. Kwong, C.-C. Liu, J. Gould, L. Hood, and J.R. Heath, Integrated barcode chips for rapid, multiplexed analysis of proteins in microliter quantities of blood. Nature Biotechnology, 2008. 26(12): p. 1373-1378.
66. Bohm, K.J., R. Stracke, M. Baum, M. Zieren, and E. Unger, Effect of temperature on kinesin-driven microtubule gliding and kinesin ATPase activity. Febs Letters, 2000. 466(1): p. 59-62.
67. Bohm, K.J., R. Stracke, and E. Unger, Speeding up kinesin-driven microtubule gliding in vitro by variation of cofactor composition and physicochemical parameters. Cell Biology International, 2000. 24(6): p. 335-341.
68. Greene, A.C., A.M. Trent, and G.D. Bachand, Controlling kinesin motor proteins in nanoengineered systems through a metal-binding on/off switch. Biotechnology and Bioengineering, 2008. 101(3): p. 478-486.
69. Grant, B.J., R.A. Cross, and J.A. McCammon, Electrostatically Biased Binding of Kinesin to Microtubules. Biophysical Journal, 2011. 100(3): p. 121-121.
70. Grant, B.J., J.A. McCammon, L.S.D. Caves, and R.A. Cross, Multivariate analysis of conserved sequence-structure relationships in kinesins: Coupling of the active site and a tubulin-binding sub-domain. Journal of Molecular Biology, 2007. 368(5): p. 1231-1248.

71. Lin, C.-T., M.-T. Kao, E. Meyhofer, and K. Kurabayashi, Surface landing of microtubule nanotracks influenced by lithographically patterned channels. Applied Physics Letters, 2009. 95(10).
72. Lin, C.-T., E. Meyhofer, and K. Kurabayashi, Predicting the stochastic guiding of kinesin-driven microtubules in microfabricated tracks: A statistical-mechanics-based modeling approach. Physical Review E, 2010. 81(1).
73. Gittes, F., B. Mickey, J. Nettleton, and J. Howard, FLEXURAL RIGIDITY OF MICROTUBULES AND ACTIN-FILAMENTS MEASURED FROM THERMAL FLUCTUATIONS IN SHAPE. Journal of Cell Biology, 1993. 120(4): p. 923-934.
74. Clemmens, J., H. Hess, R. Lipscomb, Y. Hanein, K.F. Bohringer, C.M. Matzke, G.D. Bachand, B.C. Bunker, and V. Vogel, Mechanisms of microtubule guiding on microfabricated kinesin-coated surfaces: Chemical and topographic surface patterns. Langmuir, 2003. 19(26): p. 10967-10974.
75. Moorjani, S.G., L. Jia, T.N. Jackson, and W.O. Hancock, Lithographically patterned channels spatially segregate kinesin motor activity and effectively guide microtubule movements. Nano Letters, 2003. 3(5): p. 633-637.
76. Huang, Y.M., M. Uppalapati, W.O. Hancock, and T.N. Jackson, Microfabricated capped channels for biomolecular motor-based transport. Ieee Transactions on Advanced Packaging, 2005. 28(4): p. 564-570.
77. Huang, Y.-M., M. Uppalapati, W.O. Hancock, and T.N. Jackson, Microtubule transport, concentration and alignment in enclosed microfluidic channels. Biomedical Microdevices, 2007. 9(2): p. 175-184.
78. Verma, V., W.O. Hancock, and J.M. Catchmark, Nanoscale patterning of kinesin motor proteins and its role in guiding microtubule motility. Biomedical Microdevices, 2009. 11(2): p. 313-322.
79. Lin, C.T., M.T. Kao, K. Kurabayashi, and E. Meyhofer, Efficient designs for powering microscale devices with nanoscale biomolecular motors. Small, 2006. 2(2): p. 281-287.

80. Lin, C.-T., M.-T. Kao, K. Kurabayashi, and E. Meyhofer, Self-contained biomolecular motor-driven protein sorting and concentrating in an ultrasensitive microfluidic chip. Nano Letters, 2008. 8(4): p. 1041-1046.
81. Doot, R.K., H. Hess, and V. Vogel, Engineered networks of oriented microtubule filaments for directed cargo transport. Soft Matter, 2007. 3(3): p. 349-356.
82. Clemmens, J., H. Hess, R. Doot, C.M. Matzke, G.D. Bachand, and V. Vogel, Motor-protein "roundabouts": Microtubules moving on kinesin-coated tracks through engineered networks. Lab on a Chip, 2004. 4(2): p. 83-86.
83. Bachand, M., A.M. Trent, B.C. Bunker, and G.D. Bachand, Physical factors affecting kinesin-based transport of synthetic nanoparticle cargo. Journal of Nanoscience and Nanotechnology, 2005. 5(5): p. 718-722.
84. Korten, T. and S. Diez, Setting up roadblocks for kinesin-1: mechanism for the selective speed control of cargo carrying microtubules. Lab on a Chip, 2008. 8(9): p. 1441-1447.
85. Leduc, C., K. Padberg-Gehle, V. Varga, D. Helbing, S. Diez, and J. Howard, Molecular crowding creates traffic jams of kinesin motors on microtubules. Proceedings of the National Academy of Sciences of the United States of America, 2012. 109(16): p. 6100-6105.
86. Kis, A., S. Kasas, B. BabiÄ‡, A.J. Kulik, W. Benoît, G.A.D. Briggs, C. Schönenberger, S. Catsicas, and L. Forró, Nanomechanics of Microtubules. Physical Review Letters, 2002. 89(Copyright (C) 2010 The American Physical Society): p. 248101.
87. Sugita, S., T. Murase, N. Sakamoto, T. Ohashi, and M. Sato, Size sorting of kinesin-driven microtubules with topographical grooves on a chip. Lab on a Chip, 2010. 10(6): p. 755-761.
88. Stracke, R., K.J. Bohm, L. Wollweber, J.A. Tuszynski, and E. Unger, Analysis of the migration behaviour of single microtubules in electric fields. Biochemical and Biophysical Research Communications, 2002. 293(1): p. 602-609.
89. van den Heuvel, M.G.L., M.P. De Graaff, and C. Dekker, Molecular sorting by electrical steering of microtubules in kinesin-coated channels. Science, 2006. 312(5775): p. 910-914.

90. Kim, T., M.T. Kao, E.F. Hasselbrink, and E. Meyhofer, Active alignment of microtubules with electric fields. Nano Letters, 2007. 7(1): p. 211-217.
91. Uppalapati, M., Y.-M. Huang, T.N. Jackson, and W.O. Hancock, Microtubule alignment and manipulation using AC electrokinetics. Small, 2008. 4(9): p. 1371-1381.
92. Hutchins, B.M., W.O. Hancock, and M.E. Williams, Magnet assisted fabrication of microtubule arrays. Physical Chemistry Chemical Physics, 2006. 8(30): p. 3507-3509.
93. Giljohann, D.A. and C.A. Mirkin, Drivers of biodiagnostic development. Nature, 2009. 462(7272): p. 461-464.
94. Yager, P., T. Edwards, E. Fu, K. Helton, K. Nelson, M.R. Tam, and B.H. Weigl, Microfluidic diagnostic technologies for global public health. Nature, 2006. 442(7101): p. 412-418.
95. Gervais, L. and E. Delamarche, Toward one-step point-of-care immunodiagnostics using capillary-driven microfluidics and PDMS substrates. Lab on a Chip, 2009. 9(23): p. 3330-3337.
96. Goodchild, S., T. Love, N. Hopkins, and C. Mayers, *Engineering antibodies for biosensor technologies*, in *Advances in Applied Microbiology, Vol 58*, A.I.B.J.W.G.G.M.S.S. Laskin, Editor 2006. p. 185-226.
97. Altshuler, E.P., D.V. Serebryanaya, and A.G. Katrukha, Generation of recombinant antibodies and means for increasing their affinity. Biochemistry-Moscow, 2010. 75(13): p. 1584-1605.
98. Boder, E.T., K.S. Midelfort, and K.D. Wittrup, Directed evolution of antibody fragments with monovalent femtomolar antigen-binding affinity. Proceedings of teh National Academy of Sciences of the United States of America, 2000. 97(20): p. 10701-10705.
99. Bradbury, A.R.M., S. Sidhu, S. Duebel, and J. McCafferty, Beyond natural antibodies: the power of in vitro display technologies. Nature Biotechnology, 2011. 29(3): p. 245-254.
100. Chmura, A.J., M.S. Orton, and C.F. Meares, Antibodies with infinite affinity. Proceedings of the National Academy of Sciences of the United States of America, 2001. 98(15): p. 8480-8484.

101. Colby, D.W., B.A. Kellogg, C.P. Graff, Y.A. Yeung, J.S. Swers, and K.D. Wittrup, Engineering antibody affinity by yeast surface display. Protein Engineering, 2004. 388: p. 348-358.
102. Kobayashi, N., Y. Kato, H. Oyama, and J. Goto, Antibody engineering-based approach for hapten immunometric assays with high sensitivity. Yakugaku Zasshi-Journal of the Pharmaceutical Society of Japan, 2007. 127(1): p. 55-69.
103. Lippow, S.M., K.D. Wittrup, and B. Tidor, Computational design of antibody-affinity improvement beyond in vivo maturation. Nature Biotechnology, 2007. 25(10): p. 1171-1176.
104. Starwalt, S.E., E.L. Masteller, J.A. Bluestone, and D.M. Kranz, Directed evolution of a single-chain class II MHC product by yeast display. Protein Engineering, 2003. 16(2): p. 147-156.
105. van den Beucken, T., H. Pieters, M. Steukers, M. van der Vaart, R.C. Ladner, H.R. Hoogenboom, and S.E. Hufton, Affinity maturation of Fab antibody fragments by fluorescent-activated cell sorting of yeast-displayed libraries. Febs Letters, 2003. 546(2-3): p. 288-294.
106. Weaver-Feldhaus, J.M., K.D. Miller, M.J. Feldhaus, and R.W. Siegel, Directed evolution for the development of conformation-specific affinity reagents using yeast display. Protein Engineering Design & Selection, 2005. 18(11): p. 527-536.
107. Quake, S., Microfluidics: Fluid physics at the nanoliter scale. Reviews of Modern Physics, 2005. 77: p. 977-1026.
108. Song, S.Y., Y.D. Han, S.Y. Hong, K. Kim, S.S. Yang, B.-H. Min, and H.C. Yoon, Chip-based cartilage oligomeric matrix protein detection in serum and synovial fluid for osteoarthritis diagnosis. Analytical Biochemistry, 2012. 420(2): p. 139-146.
109. Matsunaga, T., Y. Maeda, T. Yoshino, H. Takeyama, M. Takahashi, H. Ginya, J. Aasahina, and H. Tajima, Fully automated immunoassay for detection of prostate-specific antigen using nano-magnetic beads and micro-poly styrene bead composites, 'Beads on Beads'. Analytica Chimica Acta, 2007. 597(2): p. 331-339.

110. Scientific, T., Automated Magnetic Separations for Proteomics, P.P.B. Products, Editor 2012, Thermo Fisher Scientific Inc.: Rockford.
111. Healthcare, G. *Biacore*. 2012 [cited 2011 September 14].
112. *RDTinfo: Current Information on Rapid Diagnostic Tests*. 2008 [cited 2011 September 14]; http://www.rapid-diagnostics.org/technologies.htm%5D.
113. Schutzer, S.E., T. Liu, B.H. Natelson, T.E. Angel, A.A. Schepmoes, S.O. Purvine, K.K. Hixson, M.S. Lipton, D.G. Camp, II, P.K. Coyle, R.D. Smith, and J. Bergquist, Establishing the Proteome of Normal Human Cerebrospinal Fluid. PLoS ONE, 2010. 5(6): p. e10980.
114. Anderson, N. and N. Anderson, The human plasma proteome: history, character, and diagnostic prospects. Mol Cell Proteomics, 2002. 1(11): p. 845-67.
115. Manuel, Y., J.P. Revillard, and H. Betuel, *Proteins in Normal and Pathological Urine*1970, Baltimore and Manchester: University Park Press.
116. Yoshizawa, J.M., C.A. Schafer, J.J. Schafer, J.J. Farrell, B.J. Paster, and D.T. Wong, Salivary biomarkers: toward future clinical and diagnostic utilities. Clin Microbiol Rev, 2013. 26(4): p. 781-91.
117. Rasia, M. and A. Bollini, Red blood cell shape as a function of medium,Äôs ionic strength and pH. Biochimica et Biophysica Acta (BBA) - Biomembranes, 1998. 1372(2): p. 198-204.
118. Korten, S., N. Albet-Torres, F. Paderi, L.t. Siethoff, S. Diez, T. Korten, G.t. Kronnie, and A. Mansson, Sample solution constraints on motor-driven diagnostic nanodevices. Lab Chip, 2013. 13(5): p. 866-76.
119. Lee, W.G., Y.-G. Kim, B.G. Chung, U. Demirci, and A. Khademhosseini, Nano/Microfluidics for diagnosis of infectious diseases in developing countries. Advanced Drug Delivery Reviews, 2010. 62(4-5): p. 449-457.
120. Rosen, Y. and P. Gurman, MEMS and Microfluidics for Diagnostics Devices. Current Pharmaceutical Biotechnology, 2010. 11(4): p. 366-375.
121. Barradas, R.G., S. Fletcher, and J.D. Porter, The hydrolysis of maleimide in alkaline solution. Canadian Journal of Chemistry, 1976. 54(9): p. 1400-1404.
122. Scientific, T., Instructions 2-Mercaptoethylamine HCl, P. Biotechnology, Editor: Rockford.

123. Hermanson, G.T., *Bioconjugate Techniques*. Second ed2008, London: Elsevier.
124. Curtis, R.A. and L. Lue, A molecular approach to bioseparations: Protein-protein and protein-salt interactions. Chemical Engineering Science, 2006. 61(3): p. 907-923.
125. Abul Abbas, A.L., Shiv Pillai, *Cellular and Molecular Immunology*. 7th ed2012, Philadelphia: Elsevier Inc.
126. Castoldi, M. and A.V. Popova, Purification of brain tubulin through two cycles of polymerization-depolymerization in a high-molarity buffer. Protein Expression and Purification, 2003. 32(1): p. 83-88.
127. Lakamper, S. and E. Meyhofer, The E-hook of tubulin interacts with kinesin's head to increase processivity and speed. Biophysical Journal, 2005. 89(5): p. 3223-3234.
128. Stirling, P.C., V.F. Lundin, and M.R. Leroux, Getting a grip on non-native proteins. Embo Reports, 2003. 4(6): p. 565-570.
129. Phizicky, E.M. and S. Fields, PROTEIN-PROTEIN INTERACTIONS - METHODS FOR DETECTION AND ANALYSIS. Microbiological Reviews, 1995. 59(1): p. 94-123.
130. Sreebny, L.M., STUDIES OF SALIVARY GLAND PROTEASES*. Annals of the New York Academy of Sciences, 1960. 85(1): p. 182-188.
131. Yu, Z., G. Kastenmv°ller, Y. He, P. Belcredi, G. Mv∂ller, C. Prehn, J. Mendes, S. Wahl, W. Roemisch-Margl, U. Ceglarek, A. Polonikov, N. Dahmen, H. Prokisch, L. Xie, Y. Li, H.E. Wichmann, A. Peters, F. Kronenberg, K. Suhre, J. Adamski, T. Illig, and R. Wang-Sattler, Differences between Human Plasma and Serum Metabolite Profiles. PLoS ONE, 2011. 6(7): p. e21230.
132. Ponsel, D., J. Neugebauer, K. Ladetzki-Baehs, and K. Tissot, High Affinity, Developability and Functional Size: The Holy Grail of Combinatorial Antibody Library Generation. Molecules, 2011. 16(5): p. 3675-3700.
133. Mock Dm and Malik Mi, Distribution of biotin in human plasma: most of the biotin is not bound to protein. (0002-9165 (Print)).

134. Kawamura, R., A. Kakugo, Y. Osada, and J.P. Gong, Microtubule bundle formation driven by ATP: the effect of concentrations of kinesin, streptavidin and microtubules. Nanotechnology, 2010. 21(14).
135. Scott, C.W., A.B. Klika, M.M.S. Lo, T.E. Norris, and C.B. Caputo, Tau protein induces bundling of microtubules in vitro: Comparison of different tau isoforms and a tau protein fragment. Journal of Neuroscience Research, 1992. 33(1): p. 19-29.
136. Sanchez, T. and Z. Dogic, *Engineering Oscillating Microtubule Bundles*, in *Cilia, Pt A*, W.F. Marshall, Editor 2013. p. 205-224.
137. Liu, Y., Y. Guo, J.M. Valles, and J.X. Tang, Microtubule bundling and nested buckling drive stripe formation in polymerizing tubulin solutions. Proceedings of the National Academy of Sciences, 2006. 103(28): p. 10654-10659.
138. Kurz Jc and Williams Rc, Jr., Microtubule-associated proteins and the flexibility of microtubules. (0006-2960 (Print)).
139. Thavasu, P., S. Longhurst, S. Joel, M. Slevin, and F. Balkwill, Measuring cytokine levels in blood. Importance of anticoagulants, processing, and storage conditions. Journal of Immunological Methods, 1992. 153(1-2): p. 115-24.
140. Kerssemakers, J., J. Howard, H. Hess, and S. Diez, The distance that kinesin-1 holds its cargo from the microtubule surface measured by fluorescence interference contrast microscopy. Proceedings of the National Academy of Sciences, 2006. 103(43): p. 15812-15817.
141. Ray, S., E. Meyh√∂fer, R.A. Milligan, and J. Howard, Kinesin follows the microtubule's protofilament axis. The Journal of Cell Biology, 1993. 121(5): p. 1083-1093.
142. Iwatani, S., A.H. Iwane, H. Higuchi, Y. Ishii, and T. Yanagida, Mechanical and Chemical Properties of Cysteine-Modified Kinesin Molecules. Biochemistry, 1999. 38(32): p. 10318-10323.
143. Foley, J.O., K.E. Nelson, A. Mashadi-Hossein, B.A. Finlayson, and P. Yager, Concentration Gradient Immunoassay. 2. Computational Modeling for Analysis and Optimization. Analytical Chemistry, 2007. 79(10): p. 3549-3553.

144. Morozov, V.N. and T.Y. Morozova, Active bead-linked immunoassay on protein microarrays. Analytica Chimica Acta, 2006. 564(1): p. 40-52.
145. Diehl, M.R., K. Zhang, H.J. Lee, and D.A. Tirrell, Engineering Cooperativity in Biomotor-Protein Assemblies. Science, 2006. 311(5766): p. 1468-1471.